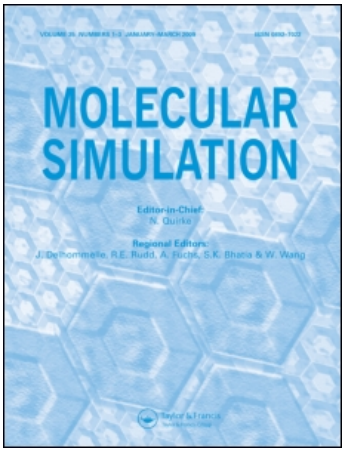

Molecular Simulation
Publication details, including instructions for authors and subscription information:
http://www.informaworld.com/smpp/title~content=t713644482

A Very Precise Canonical Ensemble Monte Carlo Determination of Thermodynamic Properties and of Radial Distribution Functions and Electric Potentials Around Ions in a Primitive Model of 2M Mixtures of KCl and KF at 25°C

Torben Smith Sørensen[a]
[a] Institute of Physical Chemistry and Center for Modelling, Nonlinear Systems Dynamics and Irreversible Thermodynamics, Technical University of Denmark, Vanløse, Denmark

To cite this Article Sørensen, Torben Smith(1995) 'A Very Precise Canonical Ensemble Monte Carlo Determination of Thermodynamic Properties and of Radial Distribution Functions and Electric Potentials Around Ions in a Primitive Model of 2M Mixtures of KCl and KF at 25°C', Molecular Simulation, 14: 2, 83 — 123
To link to this Article: DOI: 10.1080/08927029508022009
URL: http://dx.doi.org/10.1080/08927029508022009

Molecular Simulation, 1995, Vol. 14, pp. 83–123
Reprints available directly from the publisher
Photocopying permitted by license only

A VERY PRECISE CANONICAL ENSEMBLE MONTE CARLO DETERMINATION OF THERMODYNAMIC PROPERTIES AND OF RADIAL DISTRIBUTION FUNCTIONS AND ELECTRIC POTENTIALS AROUND IONS IN A PRIMITIVE MODEL OF 2 M MIXTURES OF KCl AND KF AT 25°C

TORBEN SMITH SØRENSEN

Institute of Physical Chemistry and Center for Modelling, Nonlinear Systems Dynamics and Irreversible Thermodynamics, Technical University of Denmark, Nørager Plads 3, DK2720 Vanløse, Denmark

(Received July 1994, accepted July 1994)

Long-run Canonical Ensemble Monte Carlo Simulations (up to 30 million configurations) of a primitive model KCl–KF electrolyte mixture at a total concentration 2 M and at 25°C have been performed for a wide range of the number of ions (N) in the simulation cell (from $N = 16$ up to $N = 1728$) and for a number of ratios between the two salt concentrations. The excess energy, the excess heat capacity and the single ion activity coefficients have been simulated directly. The excess osmotic pressure is calculated as a function of salt fraction. A pseudo-ideal point is found for a specific salt fraction, where the osmotic pressure has the ideal van't Hoff value. The previously found analytical correction of the Widom method for the deviation from electroneutrality is used for the single ion activity coefficients. Single "ion" activity coefficients are also simulated for "ions" of the same sizes, but without charge. The results are compared to Mean Spherical Approximation and to Carnahan-Starling-Mansoori calculations and to previous MC results for 1 M total concentration. Harned linearity in the salt fraction is found for all thermodynamic quantities. The results are discussed in the light of the theories of specific interactions of ions of Brønsted and Guggenheim. The radial distribution functions have also been simulated. From these are calculated the potentials of mean forces between the ions and the electric potential around ions. The latter may be derived from a Debye–Hückelian differential equation with an individual effective screening length for each ion (shorter than the Debye length).

KEY WORDS: Canonical ensemble Monte Carlo, KCl–KF mixtures, excess energy, heat capacity, single ion activities, osmotic pressure, extended Harned rules, radial distribution functions, potential of mean forces, electric potential, individual screening lengths, MSA theory.

INTRODUCTION

In three previous papers [1–3], canonical ensemble Monte Carlo simulations were reported for primitive model KCl–KF mixtures at 25°C and 1 M total concentration. The (hydrated) ionic diameters of the K^+ ion and the Cl^- ion were both set equal to 0.29 nm, and the diameter of the hydrated F^- ion were set equal to either 0.34 nm ("normal" system) or equal to 0.37 nm ("exaggerated" system). The basic procedure was the Metropolis/Minimum Image method used by Card and Valleau [4] supplemented by simultaneous simulation of the single ion excess chemical potential by the "test

particle" method of Widom [5–6]. The analytical correction formula for the deviation from electroneutrality, when a single ionic species is introduced, which were derived in ref. [7], was used in ref. [2] (but not in ref. [1]). The radial distribution functions (RDF) were also simulated, and from these the potentials of mean forces between ions and the conditional electric potentials around the ions were calculated [3]. In spite of the fact, that the Debye length is of the same order of magnitude as the ionic diameters, the potentials found were very "Debye-Hückelian".

In the present paper, the "exaggerated" KCl–KF system is simulated at 2 M total concentration in order to see some more deviation from Debye-Hückel behaviour. Simulations are performed for solutions of the pure salts, for 1:1 mixtures and for 12:1 and 1:12 mixtures. The number of ions in the simulation box is varied from $N = 16$ to $N = 1728$, and the number of configurations varies from 3 to 30 millions (highest for the higher N) in order to have nice extrapolations to the thermodynamic limit. Mixtures of "ions" without charge, but with the same sizes, are simulated parallelly, to demonstrate the pure hard sphere effects. The number of configurations are considerably higher than used previously for the 1 M systems. For most of these simulations, only ≈ 0.5 millions of configurations were used. Thus, the validity of the Harned rules of linearity in the mol fraction may be examined more closely, and Harned coefficients may be determined with greater precision.

The methodology was carefully exposed in appendices in refs. [2–3]. Thus, in the present paper, I shall pass directly to the results.

SIMULATED VALUES OF THE THERMODYNAMIC QUANTITIES

In Table 1, the simulated thermodynamic values for a 2 M KCl solution at 25°C is shown. B is the Bjerrum parameter (Bjerrum length divided by the common ion diameter = 0.29 nm, and ρ^* is the dimensionless, total ion concentration (scaled by the ionic diameter). E_{ex}/NkT is the dimensionless excess energy per ion, and $C_{V,ex}/Nk$ is the dimensionless excess heat capacity at constant volume per ion. The dimensionless excess chemical potential of the potassium ion is $\mu_{ex,K^+}/kT = \ln y_{K^+}$, where y_{K^+} is the McMillan-Mayer single ionic activity coefficient (pressure = osmotic pressure + external pressure).

Simulated values for the dimensionless excess chemical potential of the "ions" in "chargeless KCl" at 2 M (and arbitrary temperature) are also shown in Table 1 [bracketed values]. The excess energy and heat capacity are zero for such hard sphere systems, of course. Figure 1 shows E_{ex}/NkT vs. $(2/L\kappa a)^2$. We have:

$$L = (N/\rho^*)^{1/3} \tag{1}$$

$$\kappa a = (4\pi B\rho^*)^{1/2} \tag{2}$$

L is the dimensionless length of the simulation box (scaled with a), κ is the inverse Debye length, and a is the (mean) ionic diameter. The parameter $x \equiv 2/L\kappa a$ is a "distance" from the thermodynamic limit. It was shown in previous papers [2, 7–9], that the values of

Table 1 Simulated thermodynamic quantities for pure 2 M KCl at 25°C (B = 2.4605, $\rho^* = 0.05876$)

N	E_{ex}/NkT	$C_{V,ex}/Nk$		$\ln y_{K^+}$ (*test particle, uncorrected*)	$\ln y_{Cl^-}$	*Millions of configs.*
16	−0.8179	0.2084		−0.1308	−0.1303	6.0
			[0.2619]			[6.0]
32	−0.8079	0.2073		−0.2008	−0.1998	6.0
			[0.2617]			[6.0]
44	−0.8036	0.2080		−0.2280	−0.2279	6.0
			[0.2611]			[6.0]
64	−0.8004	0.2110		−0.2589	−0.2609	6.0
			[0.2614]			[6.0]
120	−0.7962	0.2137		−0.3070	−0.3058	6.0
			[0.2605]			[6.0]
216	−0.7936	0.2147		−0.3429	−0.3404	6.0
			[0.2600]			[6.0]
512	−0.7918	0.2151		−0.3849	−0.3834	9.0
			[0.2602]			[9.0]
1000	−0.7905	0.2191		−0.4165	−0.4126	12.0
			[0.2628]			[12.0]
1728	—	—		−0.4298	−0.4327	21.0
			[0.2615]			[9.0]

The values in square brackets are simulated test particle values of the excess chemical potential for chargeless, 2 M "KCl" ($B = 0$, $\rho^* = 0.05876$). The ionic diameters are both 0.29 nm ($= a$).

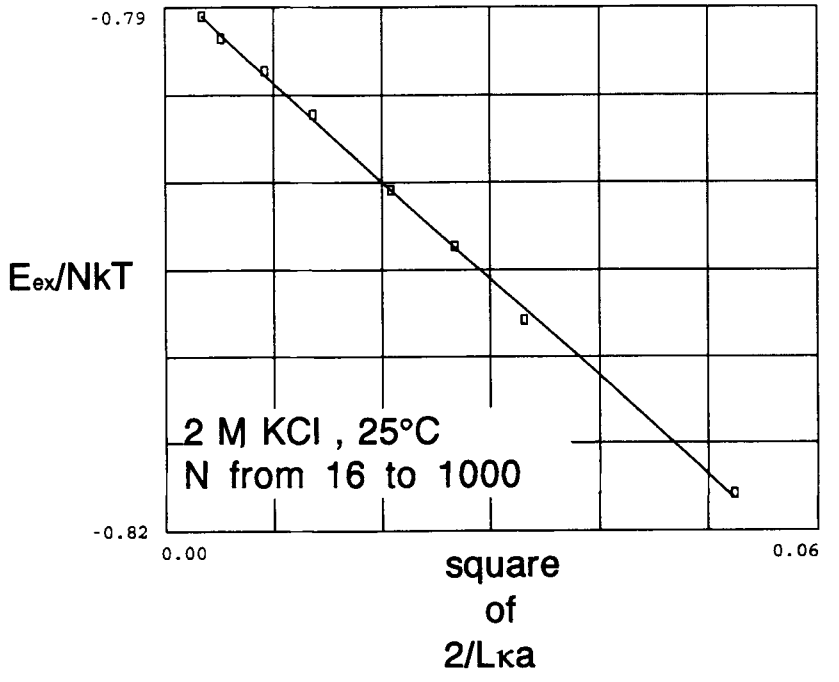

Figure 1 The dimensionless excess energy as a function of the square of the "distance from the thermodynamic limit" parameter $2/(L\kappa a)$ for a 2 M primitive model KCl solution at 25°C. The ionic diameters for both ions are 0.29 nm. $B = 2.4605$, $\rho^* = 0.05876$. The rectangles are simulated MC values, the solid line is the regression. There is perfect linearity from $N = 16$ ions to $N = 1000$ ions in the simulation cell (Pearson's $r = -0.99952$).

the excess energy and the excess heat capacity (and the corrected excess chemical potentials) relative to the values at the thermodynamic limit (infinite system with the same particle density) deviate from unity with a lowest power term proportional to x^2. In the present case Figure 1 demonstrates a perfect linearity between E_{ex}/NkT and x^2 from $N = 16$ to (at least) $N = 1000$. This corresponds to a linear plot of E_{ex}/NkT vs. $(1/N)^{2/3}$ (but not vs. $1/N$ as used by many authors). In this way, the values for the thermodynamic limit may be found with great precision. The excess heat capacity exhibits a quite good linear correlation with x^2, too, if $N = 16$ is omitted (Figure 2).

Similarly, the logarithms of the mean ionic activity coefficients (corrected to electroneutrality) seem perfectly linear against x^2 from $N = 16$ to $N = 1728$ (Figure 3). The correction of single ion excess chemical potentials are made with the formula [7]:

$$\ln y_i(\text{corr}) = \ln y_i(\text{test particle}) - B\cdot(\text{K}/[8\,L]) \tag{3}$$

$$\text{K} \equiv 12\ln(2+\sqrt{3}) - 2\pi \tag{4}$$

Figure 4 exhibits no systematic N-dependence of $\ln y$ for "chargeless" KCl. The mean value of $\ln y$ taken with N from 16 to 1728 is well in accordance with the value given by the Carnahan-Starling (pressure) as well as the Percus-Yevick (compressibility) expression, see ref. [10], Eqs. (9–18) and (9–19) specialized for one diameter

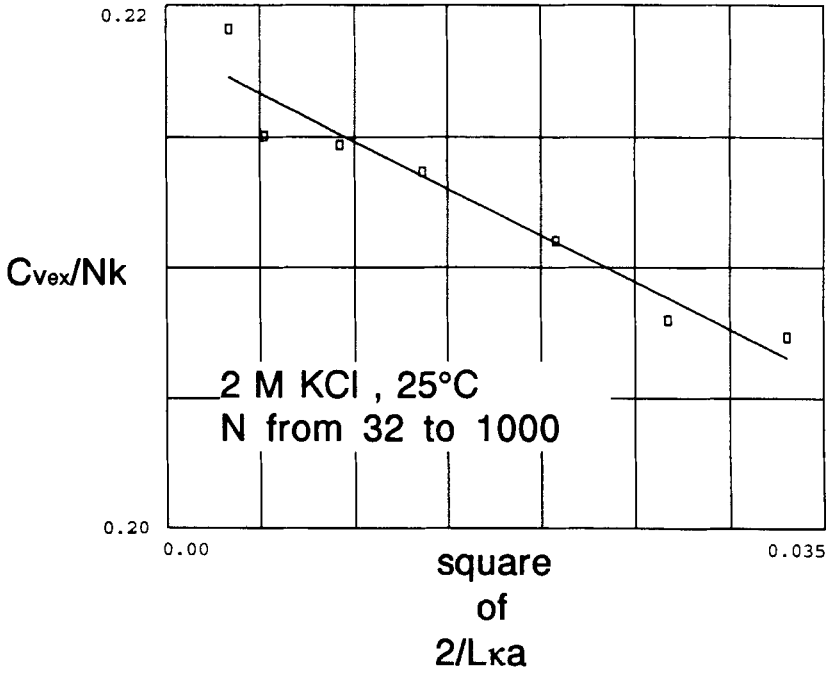

Figure 2 The dimensionless excess heat capacity at constant volume as a function of the square of $2/(L\kappa a)$ for a 2 M primitive model KCl solution at 25°C. The rectangles are simulated MC values, the solid line is the regression. There is statistical linearity from $N = 32$ ions to $N = 1000$ ions in the simulation cell, but the correlation is less good than for the excess energy ($r = -0.9652$).

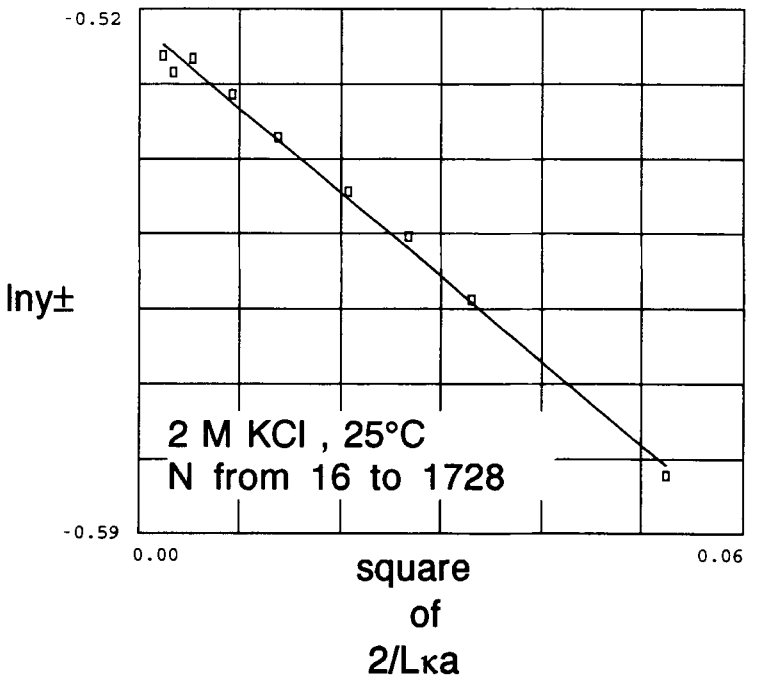

Figure 3 The values of the dimensionless excess chemical potentials (= logarithm of mean ionic activity coefficients) for the ions as a function of the square of $2/(L\kappa a)$ for a 2 M primitive model KCl solution at 25°C. The rectangles are simulated test particle values corrected to a neutralizing background. There is perfect linearity from $N = 16$ to $N = 1728$ ($r = -0.9946$).

only:

$$\ln y(CS,p) = (\eta)[3\eta^2 - 9\eta + 8]/[1-\eta]^3 \tag{5}$$

$$\ln y(PY,c) = -\ln(1-\eta) + 7[\eta/(1-\eta)] + 7.5[\eta/(1-\eta)]^2 + 3[\eta/(1-\eta)]^3 \tag{6}$$

$$\eta \equiv \pi\rho^*/6 \tag{7}$$

Table 2 and Figures 5–8 are analogous to Table 1 and Figures 1–4, but with 2 M "exaggerated" KF instead of KCl. Now, there is clearly a difference between the single ionic excess chemical potentials of the two ions with or without charge. All plots against x^2 except the ones for the excess heat capacities have linear correlation coefficients close to unity. (The heat capacities correlate less well with the present number of configurations). The extrapolations to the thermodynamic limit should be safe, with some uncertainty for the heat capacities. For two diameters (and for three ions) we have used the generalised Carnahan-Starling-Mansoori formulae as stated in the paper of Ebeling and Scherwinski [11] to calculate the hard sphere excess chemical potential, and Figure 8 shows, that the average of the simulated values of the excess chemical potentials for different N are identical to the Carnahan-Starling-Mansoori values within the statistical uncertainty.

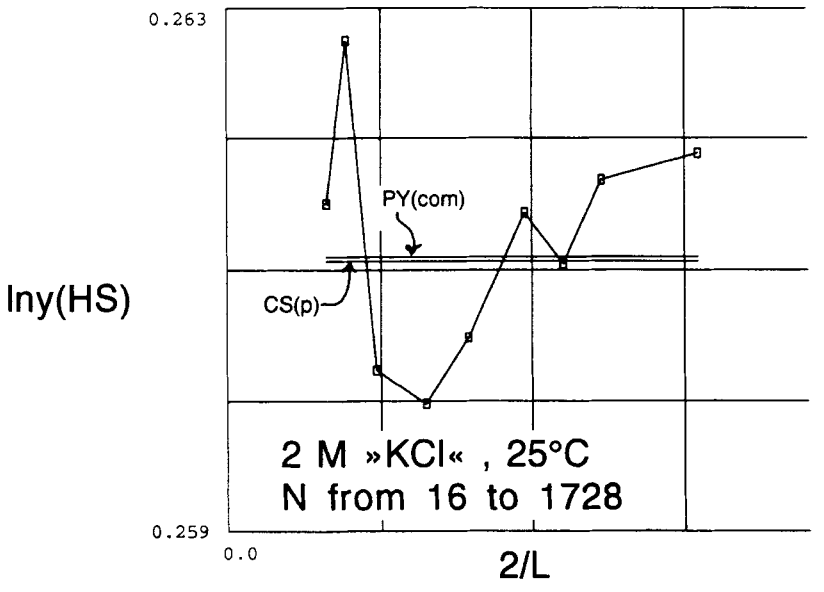

Figure 4 Test particle simulations of the dimensionless excess chemical potential in a hard sphere system of chargeless "KCl" at 2 M plotted against the hard sphere "distance from the thermodynamic limit" 2/L. The rectangles on the broken lines are the MC results. There seems to be no systematic N-dependence for N-values ranging from 16 to 1728. The values fluctuates around the value calculated from the Carnahan-Starling (pressure) or from the Percus-Yevick (compressibility) expressions. $B = 0$, $\rho^* = 0.05876$.

Table 2 Simulated thermodynamic quantities for pure 2 M KF at 25°C ($B = 2.16225$, $\rho^* = 0.08658$)

N	E_{ex}/NkT	$C_{V,ex}/Nk$	$\ln y_{K^+}$ (*test particle, uncorrected*)	$\ln y_{F^-}$	*Millions of configs.*
64	−0.7529	0.1813	−0.1064	−0.04159	7.5
			[0.3318]	[0.4812]	[7.5]
100	−0.7493	0.1860	−0.1379	−0.07467	7.5
			[0.3323]	[0.4829]	[7.5]
216	−0.7459	0.1853	−0.1880	−0.1237	7.5
			[0.3317]	[0.4823]	[7.5]
500	−0.7431	0.1901	−0.2317	−0.1696	15.0
			[0.3305]	[0.4801]	[15.0]
1000	−0.7423	0.1900	−0.2586	−0.1957	30.0
			[0.3323]	[0.4819]	[30.0]

The values in square brackets are simulated test particle values of the excess chemical potential for chargeless, 2 M "KF" ($B = 0$, $\rho^* = 0.05876$). The ionic diameters are 0.29 nm for $K^{(+)}$ and 0.37 nm for $F^{(-)}$. Mean diameter $a = 0.33$ nm.

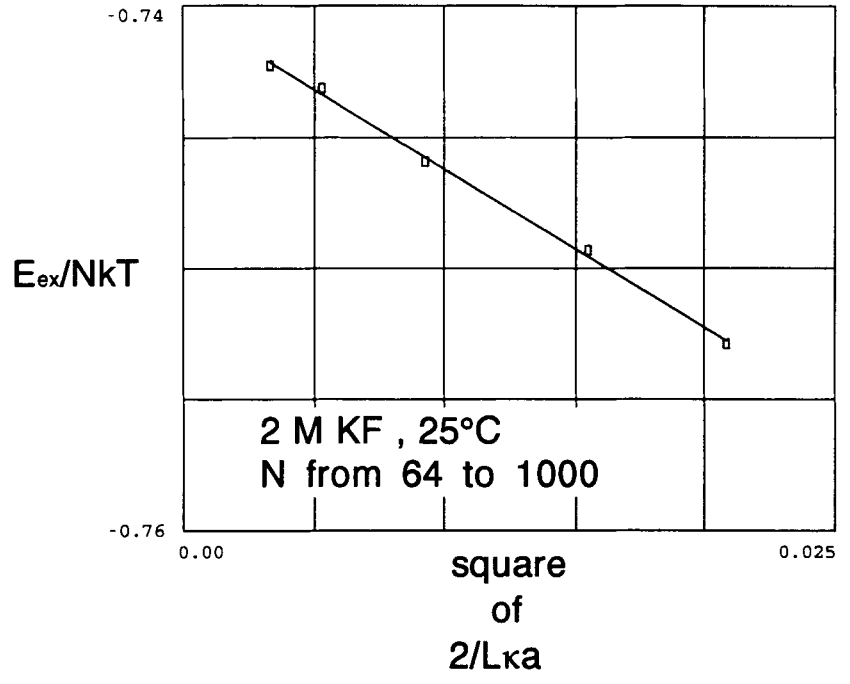

Figure 5 The dimensionless excess energy for as a function of the square of $2/(L\kappa a)$ for a 2 M primitive model KF solution at 25°C. The ionic diameters for the potassium ion is 0.29 nm and for the fluoride ion 0.37 nm. The mean diameter $a = 0.33$ nm (The size of hydrated fluoride ion is exaggerated). $B = 2.16225$, $\rho^* = 0.08658$. The rectangles are simulated MC values, the solid line is the regression. There is perfect linearity from $N = 64$ ions to $N = 1000$ ions in the simulation cell (Pearson's $r = -0.99894$).

Table 3 and Figures 9–12 correspond to an equimolar mixture of KCl and KF with a total concentration equal to 2 M. All the plots of the thermodynamic quantities vs. x^2 are linear, except the $C_{V,ex}$ plot, which is badly correlated. The extrapolated value of $C_{V,ex}$ seems to follow the Harned pattern anyway, see later. Again, the Carnahan-Starling-Mansoori values for the excess chemical potentials are within the statistical error of the simulated values for the "ions" for $B = 0$ and different N.

Finally, the Tables 4 and 5 show the results of simulations with 12 times as much KCl as KF and the opposite, respectively. The extrapolation figures are not shown for these cases. All extrapolation regressions are summarized in Table 6 in the form (TQ = thermodynamic quantity, intensive or extensive per ion):

$$\text{TQ}\ (N \text{ ions}) = \text{TQ}\ (\infty \text{ ions, same concentration}) + \alpha(2/L\kappa a)^2 \qquad (8)$$

The correlation coefficients are Pearson's r for the regressions. Most of them are very close to unity.

HARNED'S RULE AND ITS EXTENSIONS

In Figure 13a Harned's rule plot of $\ln y_{KCl}$ vs. the salt fraction of KF (X_{KF}) and of $\ln y_{KF}$ vs. the salt fraction of KCl (X_{KCl}) is shown. The excess chemical potentials for the salts are the ones extrapolated to the thermodynamic limit. Perfect linearity is exhibited:

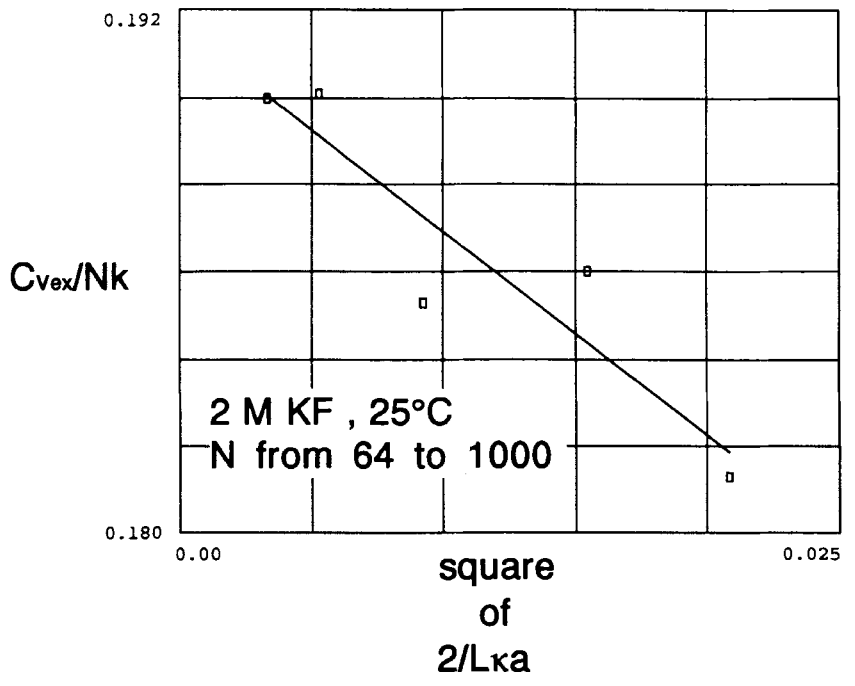

Figure 6 The dimensionless excess heat capacity at constant volume as a function of the square of $2/(L\kappa a)$ for a 2 M primitive model KF solution at 25°C. The rectangles are simulated MC values, the solid line is the regression. There is statistical linearity from $N = 64$ ions to $N = 1000$ ions in the simulation cell, but the correlation is less good ($r = -0.9247$).

Table 3 Simulated thermodynamic quantities for a 2 M 1:1 mixture of KF and KCl at 25°C ($B = 2.2533$, $\rho^* = 0.07650$)

N	E_{ex}/NkT	$C_{V,ex}/Nk$	$\ln y_{K^+}$	$\ln y_{Cl^-}$	$\ln y_{F^-}$	*Millions of configs.*
			(test particle, uncorrected)			
60	−0.7776	0.1961	−0.1784	−0.2481	−0.05331	12.0
			[0.2963]	[0.2963]	[0.4346]	[12.0]
120	−0.7724	0.1999	−0.2264	−0.2993	−0.10441	6.0
			[0.2959]	[0.2959]	[0.4337]	[6.0]
260	−0.7691	0.2045	−0.2809	−0.3520	−0.1558	6.0
			[0.2962]	[0.2962]	[0.4336]	[6.0]
500	−0.7679	0.1975	−0.3085	−0.3794	−0.1825	6.0
			[0.2951]	[0.2951]	[0.4324]	[6.0]
1000	−0.7674	0.2047	−0.3394	−0.4093	−0.2113	12.0
			[0.2970]	[0.2970]	[0.4342]	[12.0]

The values in square brackets are simulated test particle values of the excess chemical potential for chargeless, 2 M "KF + KCl" ($B = 0$, $\rho^* = 0.07650$). The ionic diameters are 0.29 nm for $K^{(+)}$ and $Cl^{(-)}$ and 0.37 nm for $F^{(-)}$. Mean diameter $a = 0.3166\ldots$ nm. N is the total number of ions, e.g. $N = 260$ corresponds to 130 $K^{(+)}$, 65 $Cl^{(-)}$ and 65 $F^{(-)}$.

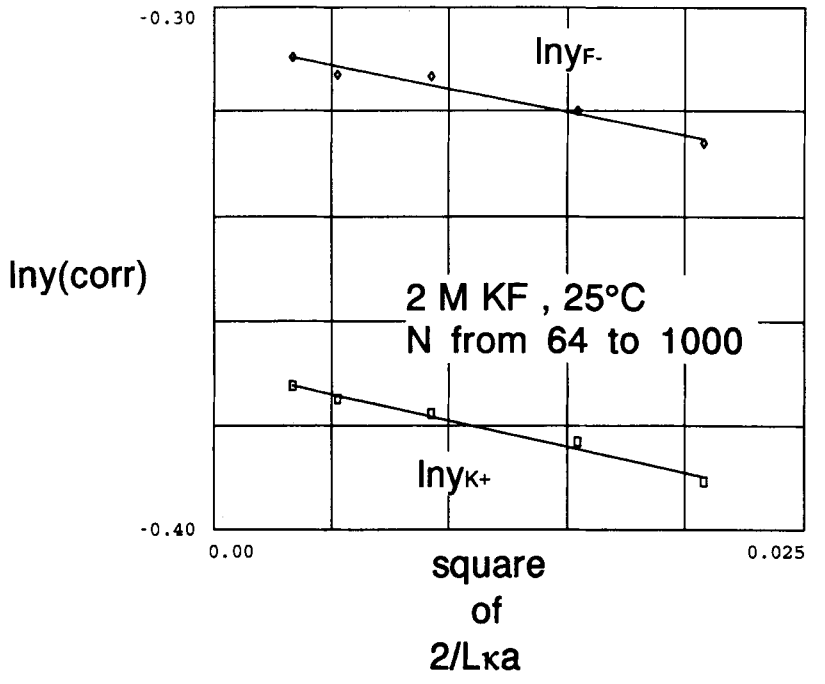

Figure 7 The values of the dimensionless excess chemical potentials (= logarithm of single ion activity coefficients) for the ions as a function of the square of $2/(L\kappa a)$ for a 2 M primitive model KF solution at 25°C. The rectangles are simulated test particle values corrected to a neutralizing background. There is perfect linearity from $N = 64$ to $N = 1000$ ($r = -0.9906$ for K^+ and $r = -0.9826$ for F^-). The extrapolated values of the single ion excess chemical potentials are clearly different for the two ions (The fluoride ion has a higher activity coefficient because of its larger volume).

Table 4 Simulated thermodynamic quantities for a 2 M mixture with KF/KCl = 1:12 at 25°C ($B = 2.2533$, $\rho^* = 0.07650$).

N	E_{ex}/NkT	$C_{V,ex}/Nk$	$\ln y_{K^+}$	$\ln y_{Cl^-}$	$\ln y_{F^-}$	*Millions of configs.*
			(test particle, uncorrected)			
52	−0.7993	0.2086	−0.2293	−0.2399	−0.05442	6.0
78	−0.7957	0.2073	−0.2652	−0.2733	−0.08717	9.0
104	−0.7933	0.2117	−0.2840	−0.2962	−0.10910	12.0
			[0.2669]	[0.2669]	[0.3956]	[12.0]
			{0.26632}	{0.26632}	{0.39444}	

The values in square brackets are simulated test particle values of the excess chemical potential for chargeless, 2 M "KF/KCl" = 1:12 ($B = 0$, $\rho^* = 0.07650$). The values in { } are Carnahan-Starling-Mansoori values. The ionic diameters are 0.29 nm for $K^{(+)}$ and $Cl^{(-)}$ and 0.37 nm for $F^{(-)}$. Mean diameter $a = 0.31666...$ nm. N is the total number of ions. The three situations correspond to 2, 3 and 4 $F^{(-)}$.

$$\ln y_{\pm,KCl} = \ln y_{\pm}(\text{pure KCl}) - \alpha^*_{KCl} X_{KF} \tag{9a}$$

$$\ln y_{\pm}(\text{pure KCl}) = -0.5254;\ \alpha^*_{KCl} = -0.0872;\ r = 0.9975 \tag{9b}$$

$$\ln y_{\pm,KF} = \ln y_{\pm}(\text{pure KF}) - \alpha^*_{KF} X_{KCl} \tag{10a}$$

$$\ln y_{\pm}(\text{pure KF}) = -0.3364;\ \alpha^*_{KF} = +0.0968;\ r = -0.99924 \tag{10b}$$

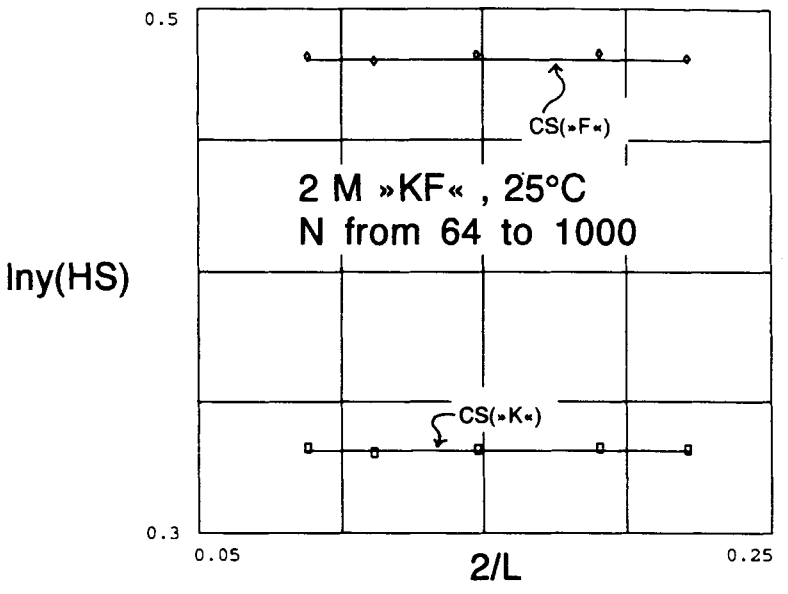

Figure 8 Test particle simulations of the dimensionless excess chemical potentials in a hard sphere system of chargeless "KF" at 2 M plotted against 2/L. The rectangles are the MC results for the chargeless "K" particle (diameter 0.29 nm) and the diamonds the MC results for the chargeless "F" particle (diameter 0.37 nm). There seem to be no N-dependence for N-values ranging from 64 to 1000. The values fluctuates around the values calculated from the Carnahan-Starling-Mansoori formula for mixtures of hard spheres (horizontal solid lines). $B = 0$, $\rho^* = 0.08658$.

Table 5 Simulated thermodynamic quantities for a 2 M mixture with KF/KCl = 12:1 at 25°C ($B = 2.2533$, $\rho^* = 0.07650$)

N	E_{ex}/NkT	$C_{V,ex}/Nk$	$\ln y_{K^+}$	$\ln y_{Cl^-}$	$\ln y_{F^-}$	*Millions of configs.*
			(test particle, uncorrected)			
52	−0.7588	0.1827	−0.10137	−0.2332	−0.02839	9.0
78	−0.7548	0.1852	−0.1315	−0.2666	−0.06061	9.0
104	−0.7528	0.1854	−0.1536	−0.2853	−0.08173	12.0
			[0.3257]	[0.3257]	[0.4735]	[9.0]
			{0.32571}	{0.32571}	{0.47330}	

The value in square brackets are simulated test particle values of the excess chemical potential for chargeless, 2 M "KF/KCl" = 12:1 ($B = 0$, $\rho^* = 0.07650$). The values in { } are Carnahan-Starling-Mansoori values. The ionic diameters are 0.29 nm for $K^{(+)}$ and $Cl^{(-)}$ and 0.37 nm for $F^{(-)}$. Mean diameter $a = 0.31666...$ nm. N is the total number of ions. The three situations correspond to 2, 3 and 4 $Cl^{(-)}$.

The trace excess chemical potentials are found inserting $X_{KF} = 1$ in Eq. (9a) and $X_{KCl} = 1$ in Eq. (10a):

$$\ln y_{\pm,KCl}(\text{trace}) = -0.4382;\ \ln y_{\pm,KF}(\text{trace}) = -0.4332 \qquad (11)$$

They are almost identical although not quite, since the uncertainty on the extrapolated excess chemical potentials are of the order of ± 0.0010 to ± 0.0020.

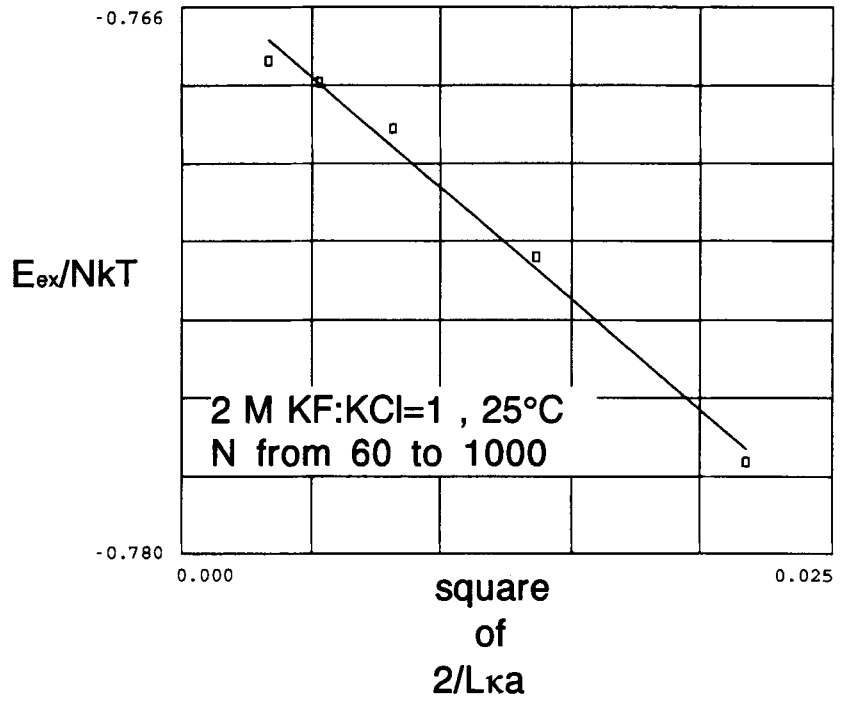

Figure 9 The dimensionless excess energy as a function of the square of $2/(L\kappa a)$ for a 2 M primitive model 1:1 mixture of KCl and KF at 25°C. The ionic diameters for the potassium ion and chloride ion are set to 0.29 nm and for the fluoride ion 0.37 nm. The mean diameter $a = 0.3166666....$ nm. $B = 2.2533$, $\rho^* = 0.07650$. The rectangles are simulated MC values, the solid line is the regression. There is perfect linearity from $N = 60$ ions to $N = 1000$ ions in the simulation cell (Pearson's $r = -0.9948$).

Equations (9–10) is an example of the original Harned's rule of linearity. However, extended linear rules are found also for the single ion excess chemical potentials and for the other thermodynamic parameters:

$$\ln y_{K^+} = -0.5252 + 0.1578\, X_{KF}(\pm 0.0005);\ r = 0.99937 \tag{12}$$

$$\ln y_{Cl^-} = -0.5304 + 0.0217\, X_{KF}(\pm 0.0020);\ r = 0.9808 \tag{13}$$

$$\ln y_{F^-} = -0.3392 + 0.0335\, X_{KF}(\pm 0.0020);\ r = 0.9984 \tag{14}$$

$$E_{ex}/NkT = -0.7880 + 0.0483\, X_{KF}(\pm 0.0010);\ r = 0.99901 \tag{15}$$

$$C_{V,ex}/Nk = +0.2167 - 0.0263\, X_{KF}(\pm 0.0020);\ r = 0.9958 \tag{16}$$

As shown in the previous tables, the test particle MC results for the excess chemical potentials for chargeless particles (called K, Cl = K and F for brevity) are quite independent of the number of particles (N) in the simulation cell. When mean values are taken for the various N's at each "salt" fraction, I obtain the following "Harned rules"

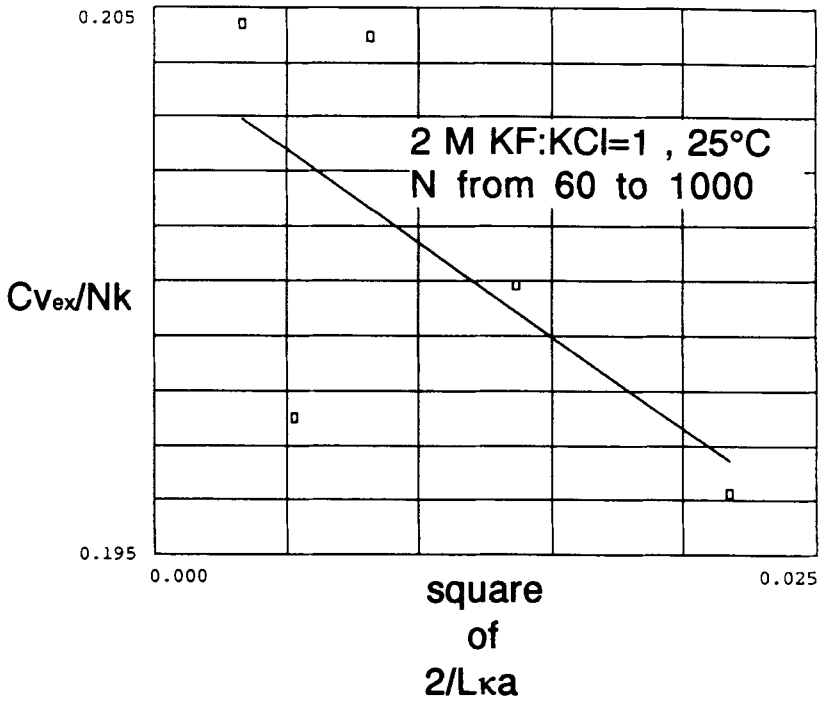

Figure 10 The dimensionless excess heat capacity at constant volume as a function of the square of $2/(L\kappa a)$ for a 2 M primitive model 1:1 mixture of KCl and KF at 25°C. The rectangles are simulated MC values, the solid line is the regression. There is no real correlation ($r = -0.641$), but nevertheless, the extrapolated value is in line with the other results (Harned linearity).

for mixtures of chargeless "ions" at 2 M total concentration:

$$\ln y_{K}(\text{HS, MC}) = 0.2613 + 0.0701\, X_{KF}(\pm 0.0010);\ r = 0.999965 \quad (5 \text{ values}) \tag{17}$$

$$\ln y_{Cl}(\text{HS, MC}) = 0.2613 + 0.0697\, X_{KF}(\pm 0.0010);\ r = 0.999987 \quad (4 \text{ values}) \tag{18}$$

$$\ln y_{F}(\text{HS, MC}) = 0.3880 + 0.0930\, X_{KF}(\pm 0.0010);\ r = 0.99986 \quad (4 \text{ values}) \tag{19}$$

HS stands for "hard spheres". Using instead the Carnahan-Starling-Mansoori formulae, the following "Harned" equations are obtained:

$$\ln y_{K \text{ or } Cl}(\text{CS}) = 0.2609 + 0.0701\, X_{KF};\ r = 0.999987 \tag{20}$$

$$\ln y_{F}(\text{CS}) = 0.3873 + 0.0931\, X_{KF};\ r = 0.999981 \tag{21}$$

It is seen, that there is every reason to believe, that the CS values at 2 M total concentration are simply the true values, around which the MC values distribute themselves randomly.

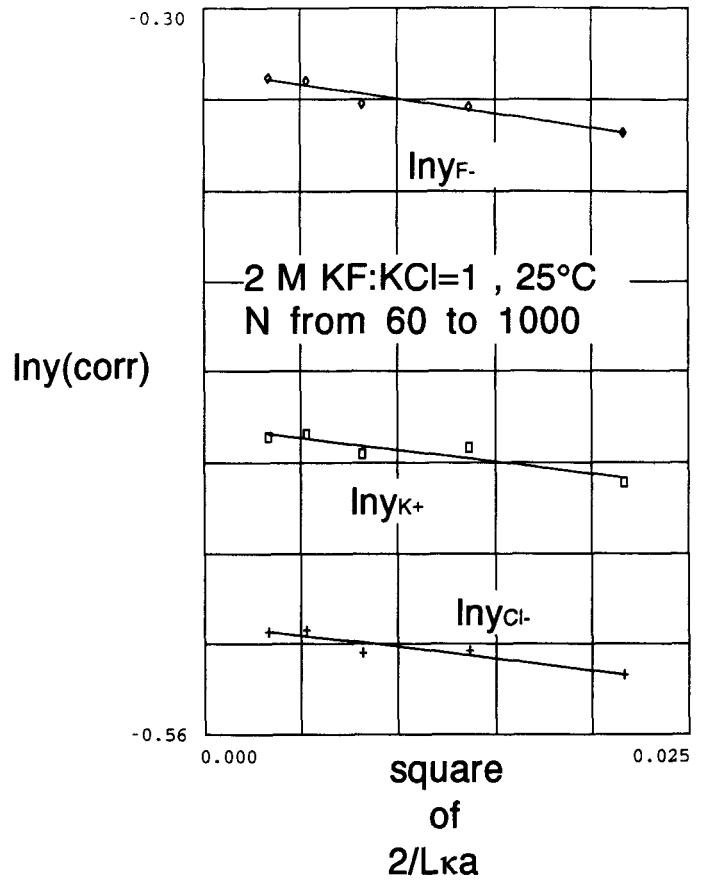

Figure 11 The values of the dimensionless excess chemical potentials (= logarithm of single ion activity coefficients) for the ions as a function of the square of $2/(L\kappa a)$ for a 2 M primitive model 1:1 mixture of KCl and KF solution at 25°C. The rectangles are simulated test particle values corrected to a neutralizing background. There are quite good linear correlations from $N = 60$ to $N = 1000$ ($r = -0.9172$ for K^+, $r = -0.9486$ for Cl^-, and $r = -0.9636$ for F^-). The extrapolated values of the single ion excess chemical potentials are clearly different for all three ions (The fluoride ion has a higher activity coefficient because of its larger volume. The potassium ion strikes a compromise between the fluoride and the chloride ion).

ELECTRIC POTENTIALS AND POTENTIALS OF MEAN FORCES

In Figure 14, the t-weighted differences of the RDF's, $t\{g_{+-}(1000) - g_{+-}(1728)\}$, in 2 M KCl are plotted vs. the dimensionless separation ($t = r/a$) in order to check if there are any systematic difference between $N = 1000$ and $N = 1728$ in the window from $t = 1$ to $t = 4$. The belt between the two + + + + + lines is the mean difference $\pm$ the standard deviation. Zero deviation is well inside this belt, so that any systematic deviation between the two RDF's is statistical insignificant. The same is shown for $t\{g_A(1000) - g_A(1728)\}$ in Figure 15. The suffix "A" stands for + + or − −.

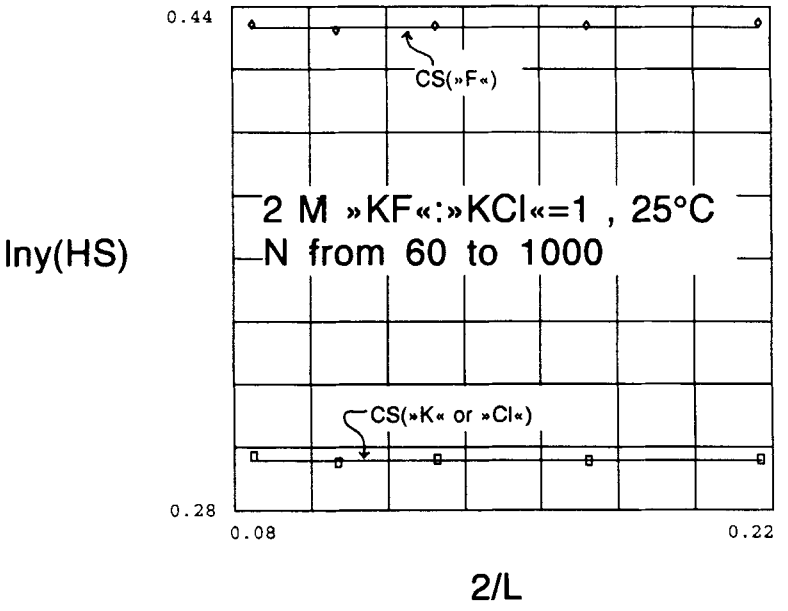

Figure 12 Test particle simulations of the dimensionless excess chemical potentials in a hard sphere system of chargeless "KF" mixed with chargeless "KCl" (1:1) at 2 M total salt concentration plotted against 2/L. The rectangles are the MC results for the chargeless "K" particle or the chargeless "Cl" particle (both with diameters 0.29 nm) and the diamonds the MC results for the chargeless "F" particle (diameter 0.37 nm). There seems to be no N-dependence for N-values ranging from 60 to 1000. The values fluctuate around the values calculated from the Carnahan-Starling-Mansoori formula for mixtures of hard spheres (horizontal solid lines). $B = 2.2533$, $\rho^* = 0.07650$.

Table 6 Summary of regressions for the thermodynamic quantities

KF:KCl	*Quantities for* $N = \infty$	α	*Pearson's r*
0	$E_{ex}/NkT = -0.78868$	−0.56269	−0.99952
	$C_{V,ex}/Nk = 0.2185$	−0.3620	−0.9652 (omission of $N = 16$)
	$\ln y_{\pm}$(corr) = −0.5228	−1.0982	−0.9946
1:12	$E_{ex}/NkT = -0.78314$	−0.67870	−0.99910
	$C_{V,ex}/Nk = 0.2146$	−0.2827	−0.558
	$\ln y_{K^+}$(corr) = −0.5140	−0.8737	−0.9327
	$\ln y_{Cl^-}$(corr) = −0.5253	−0.7695	−0.9871
	$\ln y_{F^-}$(corr) = −0.3368	−0.9429	−0.9974
1:1	$E_{ex}/NkT = -0.76493$	−0.57027	−0.9948
	$C_{V,ex}/Nk = 0.2041$	−0.3400	−0.641
	$\ln y_{K^+}$(corr) = −0.4493	−0.8464	−0.9172
	$\ln y_{Cl^-}$(corr) = −0.5203	−0.8406	−0.9486
	$\ln y_{F^-}$(corr) = −0.3224	−1.0076	−0.9636
12:1	$E_{ex}/NkT = -0.74249$	−0.67932	−0.99938
	$C_{V,ex}/Nk = 0.1906$	−0.3214	−0.9563
	$\ln y_{K^+}$(corr) = −0.3763	−1.2453	−0.9870
	$\ln y_{Cl^-}$(corr) = −0.5102	−1.1873	−0.9825
	$\ln y_{F^-}$(corr) = −0.3073	−1.0877	−0.99971
∞	$E_{ex}/NkT = -0.74011$	−0.6091	−0.99894
	$C_{V,ex}/Nk = 0.1916$	−0.4683	−0.9247
	$\ln y_{K^+}$(corr) = −0.3690	−1.0058	−0.9906
	$\ln y_{F^-}$(corr) = −0.3067	−0.8973	−0.9826

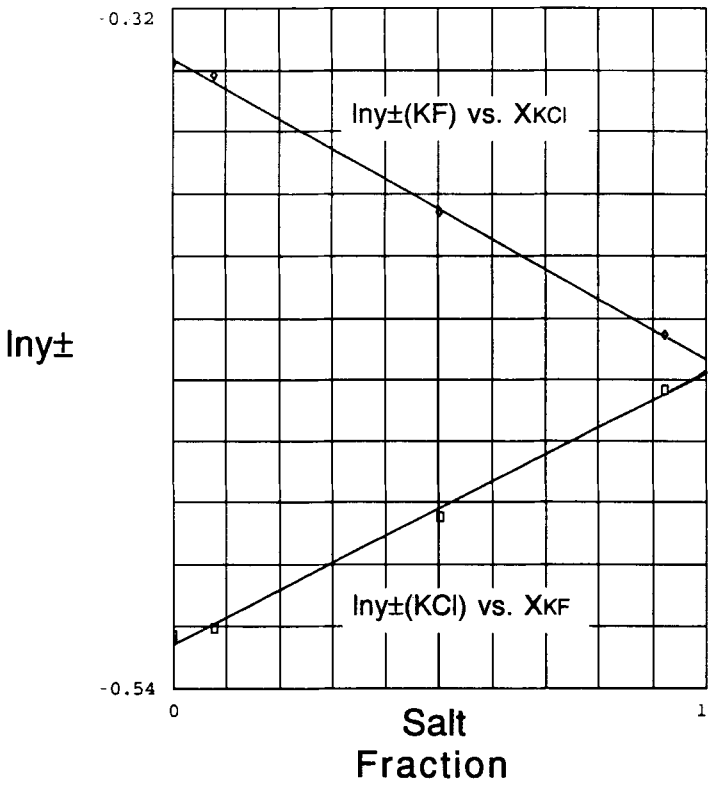

Figure 13 Harned plots of $\ln y_{\pm}$(KF) as a function of the salt fraction of KCl in the mixture and of $\ln y_{\pm}$(KCl) as a function of the salt fraction of KF. Total ionic strength = 2 M. 25°C. The logarithms of the trace activity coefficients are almost equal and almost equal to the mean value of the logarithms of the activity coefficients for the pure solutions of the two salts (almost a Guggenheim situation, see the discussion).

The (dimensionless) potentials of mean forces between the ions are found from:

$$W_{+-}(t) = -\ln g_{+-}(t) \tag{22a}$$

$$W_A(t) = -\ln g_A(t) \tag{22b}$$

For 2 M KCl these potentials of mean forces multiplied by t are shown in Figures 16–17 (as rectangles). The + + + + curves are the DHX potentials of mean forces:

$$tW_{+-}(t) = (-B)\exp(\kappa a)[1+\kappa a]^{-1}\exp(-\kappa at) \tag{23a}$$

$$tW_A(t) = (+B)\exp(\kappa a)[1+\kappa a]^{-1}\exp(-\kappa at) \tag{23b}$$

The diamonds in Figures 16–17 are the potentials of mean forces "corrected" for the potentials of mean forces in a similar, chargeless hard sphere system:

$$W^{el}_{+-}(t) = W_{+-}(t) - W^{HS}_{+-}(t) \tag{24a}$$

$$W^{el}_A(t) = W_A(t) - W^{HS}_A(t) \tag{24b}$$

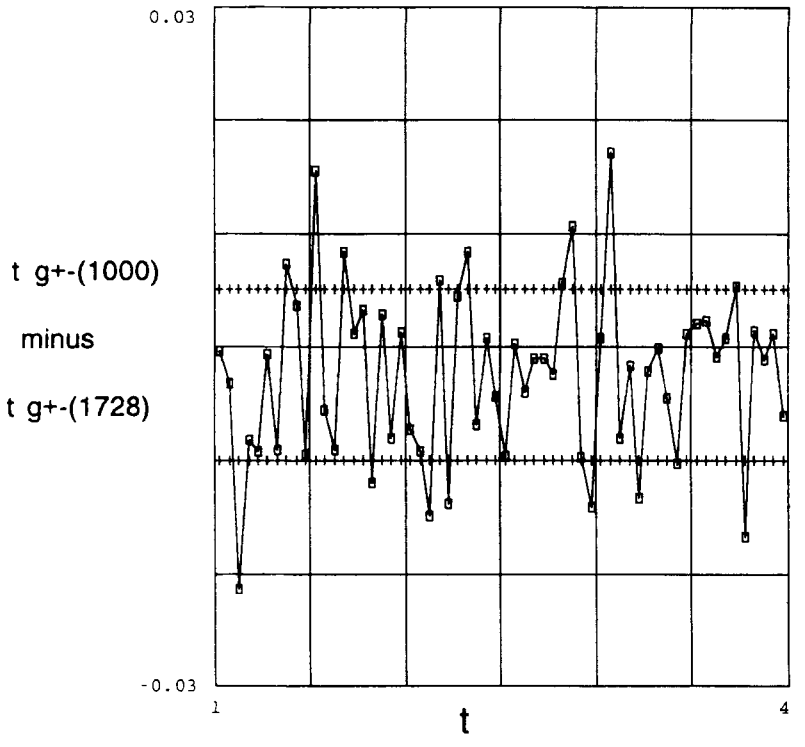

Figure 14 In order to check if there is any systematic N-dependence left in the radial distribution function g_{+-}, the differences (weighted by $t = r/a$) between values obtained with 1000 ions and with 1728 ions in the simulation cell are plotted *vs.* t for a 2 M KCl solution. The standard error belt (between the + + + + horizontal lines) clearly engulfs the zero difference, so there is no systematic N-dependence discernible.

$W^{HS}_{+-}(t)$ and $W^{HS}_{A}(t)$ are distinguished, since the same programme is used with $B = 0$. Thus, in $g^{HS}_{A}(t)$ the selected ions are missing in the countings, and these values are slightly lower than $g^{HS}_{+-}(t)$ at the higher t-values in finite box systems. The same systematic difference is expected between $g_A(t)$ and $g_{+-}(t)$. The difference should not be visible in the "electric part" of the potential of mean forces, when the differences are made according to (24a–b).

In 1 M KCl/KF (exaggerated) mixtures, the potentials of mean forces minus the potential of mean forces for the chargeless hard sphere system were found to lie very close to the DHX potential of mean forces. Between two ions (i and j) of different sizes, the Eqs. (23a–b) were generalized by replacing $\exp(\kappa a)/[1 + \kappa a]$ by $\exp(\kappa a_{ij})/[1 + \kappa a_{ij}]$ (generalized DHX). Figures 29–34 in ref. [2] exhibit this very nice correspondence. However, at a total concentration = 2 M this simple picture is no longer valid. Figure 16 shows, that the "hard sphere frce" near contact correct the potential of mean forces $W_{+-}(t)$ in the direction of DHX (compare diamonds and + + +), but the "electric part" of the potential of mean forces (diamonds) does not really coincide with the DHX (+ + +). However, the DHX is surprisingly close even in this sitation with a Debye length which is only ≈ 0.74 of the ionic diameter. Figure 17 shows, that in the case of $W_A(t)$, the "hard sphere forces" near contact "correct" to the wrong side, so that DHX

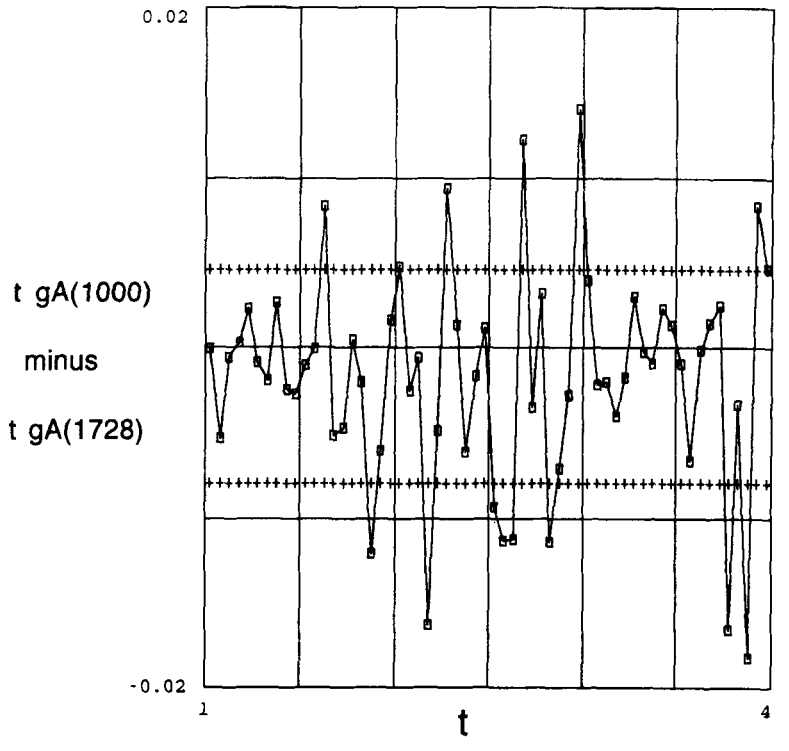

Figure 15 The same kind of scatter plot as in Figure 14, but for $g_A = g_{KK} = g_{ClCl}$. No systematic N-dependence discernible.

(+ + +) is even worse for $W_A^{el}(t)$ than for $W_A(t)$. Although the DHX values represent a fair average of the simulated values for the interactions between equally as well as between oppositely charged ions, it is generally seen, that the simulated interactions approach zero much faster in the "tails" than the DHX values. Since Figures 14–15 show that the simulated values with 1000 and with 1728 ions are statistically identical (at least) up to four diameters of separation, the simulated values are the true ones.

In ref. [3] it was shown, that the conditional electric potential around ions were very often excellently reproduced by the Debye–Hückel potential, not only for dilute systems of 1:1 electrolytes (with equal or different ionic diameters) and 2:1 electrolytes, but also for 1 M mixtures of KCl and KF. In the case of 2 M KCl, this simplicity is lost. Figure 18 shows the calculated electric potentials (rectangles) around a K^+ ion (or the negative electric potential around a Cl^- ion). The potential in the outer sampling shell have been subtracted as explained in ref. [3]. The potential deviates systematically from the DH potentials (+ + + +). However, the fit with an "effective" inverse Debye length, which is a factor 1.38 larger seems very efficient (solid curve).

The dimensionless charge density around a K^+ ion $\Delta g = g_A - g_{+-}$ is shown on Figure 19 (as rectangles). The curve calculated from the DH potential and the Poisson equation is shown as + + + +. It deviates strongly from the values calculated from the simulations. Much better is the solid curve calculated from the modified DH potential

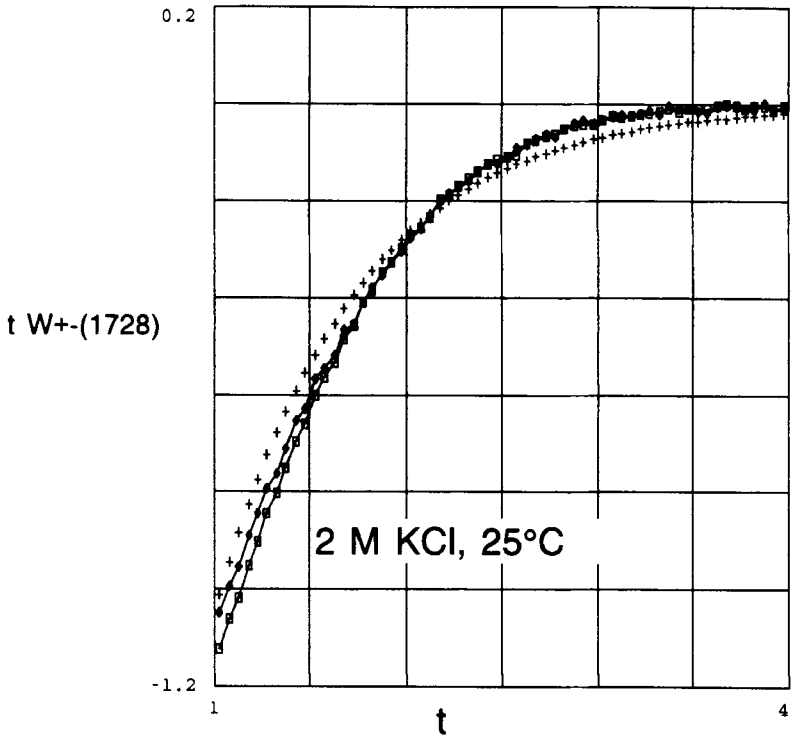

Figure 16 The dimensionless potential of mean forces (weighted by $t = r/a$) between K^+ and Cl^- in a2 M KCl from MC simulations with $N = 1728$ ions. The rectangles are MC values, the + + + + are DHX values (*i.e.* potentials of mean forces Debye-Hückelian). The diamonds are the "electric part" of the potential of mean forces (with the simulated hard sphere potential of mean forces subtracted). The "electric" potential of mean forces is near to DHX close to contact. The potential of mean forces converges more rapidly to zero than predicted by the DHX theory.

with $\kappa_{eff} = 1.38\,\kappa$, although the fit is less perfect than for the potential. It did not seem possible to make a better fit to Δg by changing κ(eff) without making worse the good fit to the potential. Thus, a modified Debye–Hückel equation

$$\nabla^2(e_0\Psi/kT) = -0.5(\kappa a)^2\Delta g \approx (\kappa_{eff}a)^2(e_0\Psi/kT) \tag{25}$$

is only partially successful (with only one eigenfunction to the Laplacian). The Laplacian in (25) is to be taken with respect to the dimensionless separation (t).

Turning now to pure 2 M KF, Figure 20 shows the potential of mean forces between a K^+ and a F^- ion multiplied by the dimensionless separation. The rectangles are the simulated values. The diamonds are the "electric" potentials of mean forces (with the simulated hard sphere "attraction" subtracted). Near contact this correction brings the simulated values very close to the DHX values (+ + + +). Again, the approach of the DHX values to zero is too slow.

In Figure 21, $t \cdot W_{KK}$ is shown (rectangles). These values deviate quite a lot from the DHX values (+ + + +) as well as from the GDHX values (× × × ×). Notice, that contact is below unity, since t is scaled by the contact distance between K^+ and F^-, and

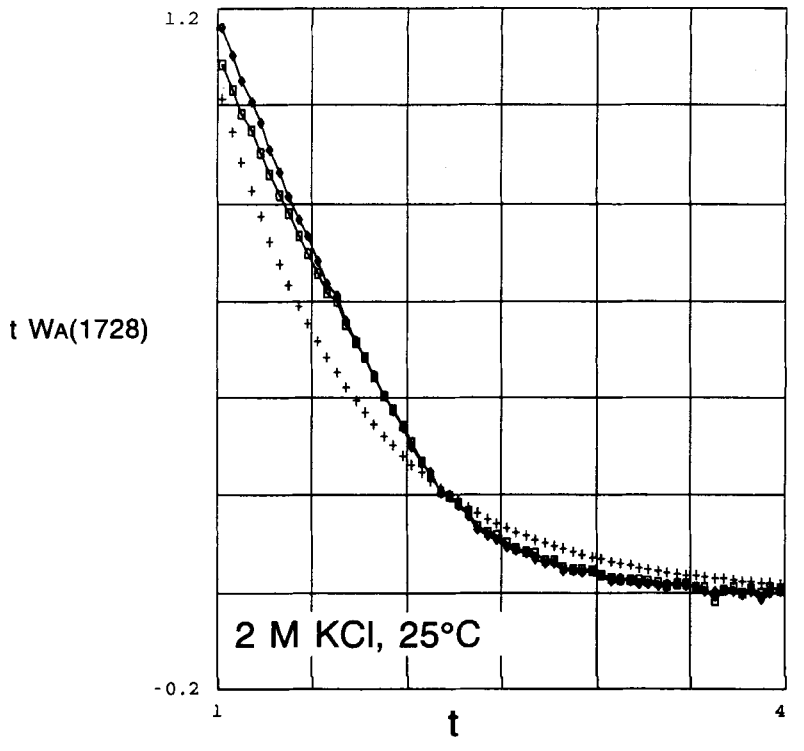

Figure 17 The dimensionless potential of mean forces (weighted by $t = r/a$) between similar ions in 2 M KCl from MC simulations with $N = 1728$ ions. The rectangles are MC values, the + + + + are DHX values. The diamonds are the "electric part" of the potential of mean forces. The "electric" potential of mean forces is more far from DHX close to contact than the total potential of mean forces (rectangles). The potential of mean forces converges more rapidly to zero than predicted by the DHX theory.

the potassium ion is smaller than the flouride ion. The "generalisation" in GDHX (replacing the contact distance a_{KF} by a_{KK} in the DHX) seems to be of dubious value in this case, since the × × × × curve are further from the rectangles as well as from the diamonds (electric potential of mean forces) than the DHX values (+ + + +). Correction for the hard sphere "attraction" is once again removing the potentials of mean forces from the DHX.

Figure 22 is similar to Figure 21, but for the interactions between two flouride ions. Notice, that the contact distance is greater than unity. In this case the GDHX values coincide (fortuituously?) with the simulated values (rectangles) near contact. There is only a slight difference between GDHX and DHX, however. The "electric" potentials of mean forces deviate appreciably from the other curves near contact. Also, the deviations of DHX and GDHX from the true values is appreciable in the tail.

Figures 23–24 show the electric potentials around a potassium ion and a fluoride ion, respectively (rectangles). The deviations from the Debye–Hückel potentials (+ + +) are appreciable – especially around the fluoride ion. The curves drawn are modified Debye–Hückel potentials with $\kappa_{eff}a = 1.27 \cdot \kappa a$ and $1.63 \cdot \kappa a$, respectively.

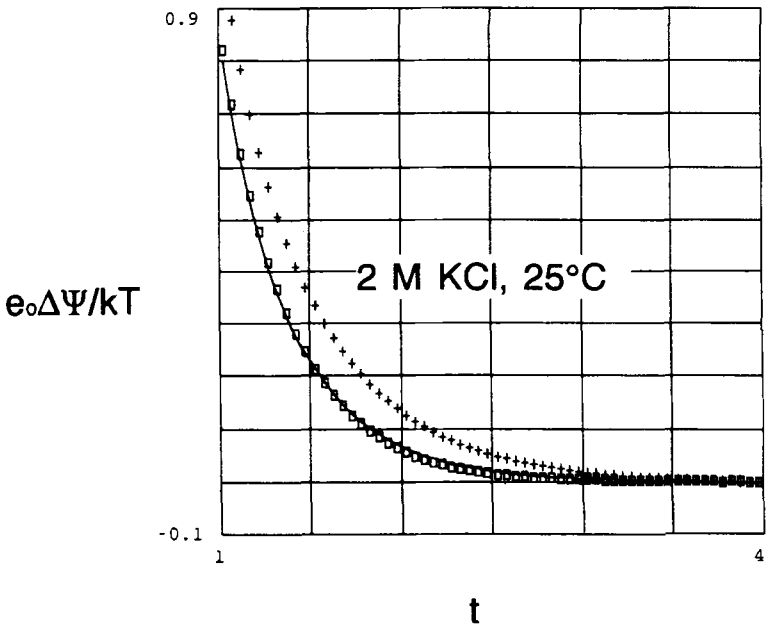

Figure 18 The dimensionless electric potential around a potassium ion (or the negative potential around a chloride ion) in 2 M KCl from MC simulations with $N = 1728$ ions. The rectangles are Poisson-integrated potentials from the simulated RDF's. Potentials are taken as differences relative to the potential at $t = r/a = 3.975$ (the mid point radius of the outermost spherical shell) but in practice, the potential here may be put to zero. The + + + + curve is the Debye-Hückel potential. The solid curve fitting the MC values quite well is calculated from a DH expression with a $\kappa_{eff} = 1.38\,\kappa$.

The potentials in Figures 23–24 have been calculated from charge densities around the ions exhibiting discontinuities as explained in ref. [3]. These near contact discontinuities are not visible in the potentials, however, since the potentials near contact are dominated by contributions from the greater charges at intermediary distances from the ions.

In a 1:1 mixture of KCl and KF there are six potentials of mean forces corresponding to the interactions KF, KCl, ClCl, KK, ClF, and FF. These potentials of mean forces are shown in Figures 25–30. Again, simulated values are shown as rectangles on broken curves. The "electric part" of the potentials of mean forces (subtracting the hard sphere interactions) are shown as diamonds on broken curves. The DHX values are denoted by + + + +, and the GDHX as × × × ×. The value of "a" in κa in DHX is the mean value of the three ionic diameters $= (0.29 + 0.29 + 0.37)/3$. This is also the value by which all separations (t) in the plots have been scaled. Similar conclusions as before may be made. In the cases, where there is really a significant difference between DHX and GDHX (such as for ClCl, KK and ClF) the GDHX is not a good deal at 2 M, since the simple DHX is closer to the simulated potentials of mean forces. Although DHX does represent a fair average for the simulated potentials, the simulated "tails" of the interactions approaches zero much faster than the DHX and GDHX values in the case of the KF and KCl interactions. For the interactions ClCl, KK and ClF the GDHX

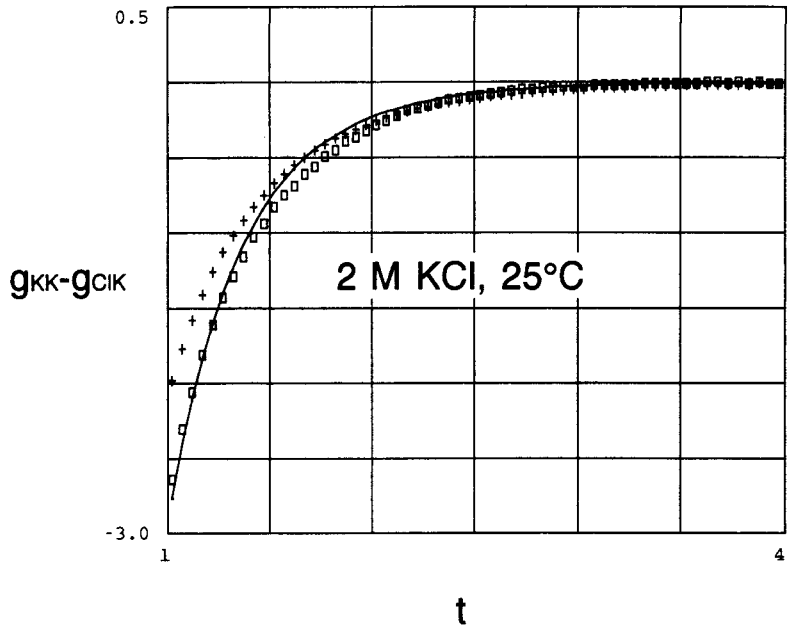

Figure 19 The dimensionless charge density around a potassium ion in 2 M KCl giving rise in the potential electric potential shown in Figure 18. The rectangles are MC values ($N = 1728$), the + + + + curve is the Debye-Hückel charge density and the solid curve corresponds to the modified DH with $\kappa_{eff} = 1.38\,\kappa$.

seems considerably better than DHX in the tail, however. For the FF interactions, both are good, but only in the tail.

The electric potentials around the ions K^+, Cl^- and F^- are shown in Figures 31–33. Again, there are appreciable deviations between the values calculated from the simulations (rectangles) and from the Debye-Hückel potential (+ + + +), but good fits are obtained with modified DH potentials with an "effective" value of κ (solid curves). Strictly speaking, it is not electric potentials, but electric potential differences which are plotted. The reference potential is the electric potential at ≈ 5.38 mean diameters. This is so far out in the "tail" of the potentials shown, that the reference potential may for all practical purposes be set to zero. The values of κ_{eff}/κ for pure KCl and KF and for 1:1 mixtures at 2 M total ionic strength are accumulated in Table 7.

THE EXCESS OSMOTIC PRESSURE

The calculation of the excess osmotic pressure (Π_{ex}) in the KCl/KF mixtures can be performed by a combination of simulated values of E_{ex}/NkT and the knowledge acquired for the RDF's at contact:

$$\Pi_{ex}/(\rho_{tot}kT) = \{\Pi/(\rho_{tot}kT)\} - 1 = E_{ex}/(3NkT) + \text{CONTACT} \tag{26}$$

$$\text{CONTACT} = (2\pi/3)\Sigma_i\Sigma_j(\rho_i/\rho_{tot})(a_{ij}/a)^3\rho_j^* g_{ij}(a_{ij}) \tag{27}$$

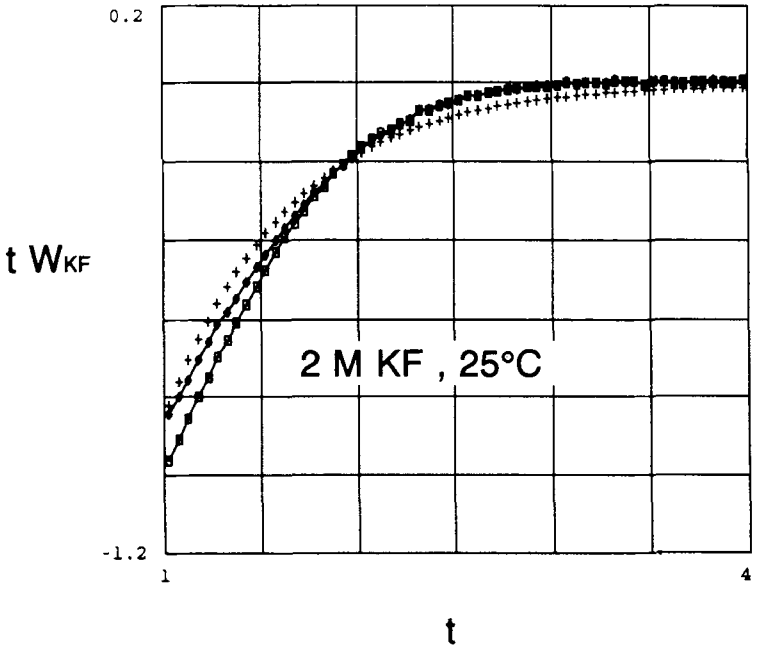

Figure 20 The dimensionless potential of mean forces (weighted by $t = r/a$) between K–F pairs in 2 M KF from MC simulations with $N = 1000$ ions. The rectangles are MC values, the + + + + are DHX values (in this case the same as the GDHX values). The diamonds are the "electric part" of the potential of mean forces. The "electric" potential of mean forces is close to DHX near contact. The potential of mean forces converges more rapidly to zero than predicted by the DHX theory. (The mean radius $a = 0.33$ nm).

Table 7 Values of κ_{eff}/κ in solutions of 2 M total ionic strength

Electrolyte	*Electric potential around...*		
	K^+	Cl^-	F^-
KCl	1.38 ± 0.03	1.38 ± 0.03	—
KF	1.27 ± 0.02	—	1.63 ± 0.03
KF/KCl = 1	1.27 ± 0.03	1.50 ± 0.05	1.33 ± 0.03

The star denotes dimensionless concentrations (ion densities multiplied by a^3, a being the mean diameter). With ρ^* being the total dimensionless concentration and g^c_{ij} being the contact values of the RDF's one obtains the following expressions (28–30).

For KCl:

$$\text{CONTACT} = \rho^*(\pi/3)\{g^c_{\text{KCl}} + g^c_{\text{A}}\} \tag{28}$$

For KF:

$$\text{CONTACT} = \rho^*(\pi/3)\{(a_{\text{KF}}/a)^3 g^c_{\text{KF}} + 0.5\cdot[(a_{\text{KK}}/a)^3 g^c_{\text{KK}} + (a_{\text{FF}}/a)^3 g^c_{\text{FF}}]\} \tag{29}$$

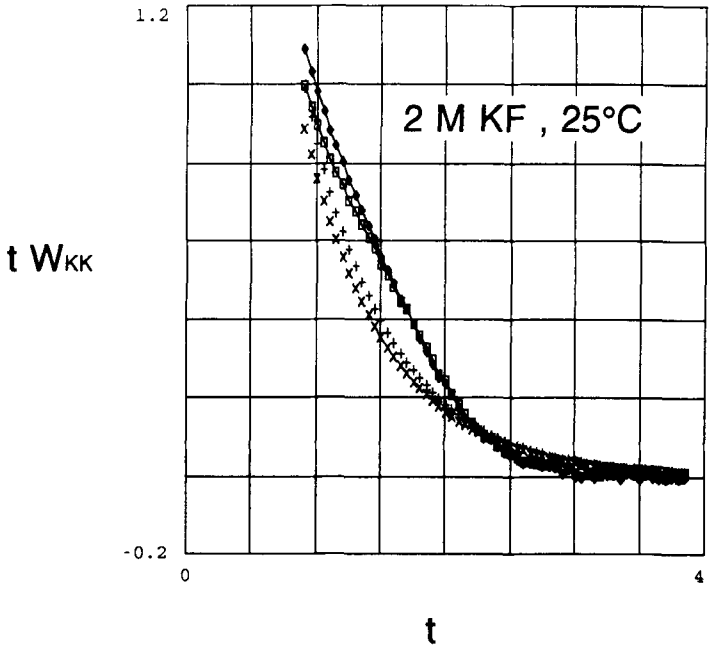

Figure 21 The dimensionless potential of mean forces (weighted by $t = r/a$) between K–K pairs in 2 M KF from MC simulations with $N = 1000$ ions. The rectangles are MC values, the + + + + are DHX values and the × × × × GDHX values. The diamonds are the "electric part" of the potential of mean forces. The "electric" potential of mean forces is further from DHX and GDHX near contact than the total potential of mean forces. The potential of mean forces converges more rapidly to zero than predicted by the (G)DHX theory.

For KCl/KF mixtures:

$$\text{CONTACT} = \rho^*(\pi/3)\{0.5\cdot[(a_{KK}/a)^3 g^c_{KK} + (a_{ClCl}/a)^3 g^c_{ClCl} X^2_{KCl} + (a_{FF}/a)^3 g^c_{FF} X^2_{KF}] + (a_{ClF}/a)^3 g^c_{ClF} X_{KCl} X_{KF} + (a_{KCl}/a)^3 g^c_{KCl} X_{KCl} + (a_{KF}/a)^3 g^c_{KF} X_{KF}\} \quad (30)$$

The last term shows, that the osmotic coefficient also have quadratic terms in the salt fraction. The values of g^c_{ij} may also vary somewhat with the salt fraction. Thus, the excess osmotic pressure should not in general be expected to obey a lineary Harned rule. In practice it does in the present case, however, as will be demonstrated, see Eq. (31).

Table 8 shows the contact values of the RDF's as determined from the simulations. Estimated uncertainties are also shown. A certain systematic variation with the salt fraction is observed. The values of the excess energy (from Eq. 15), the CONTACT term and the excess osmotic pressure are shown in Table 9. The values of the mean diameter and of the dimensionless total salt concentrations are also shown. The excess osmotic pressure obeys a perfect linear regression:

$$\Pi_{ex}/(\rho_{tot} kT) = \text{osmotic coefficient} - 1 = -0.0492 + 0.0872\, X_{KF} (r = 0.99960) \quad (31)$$

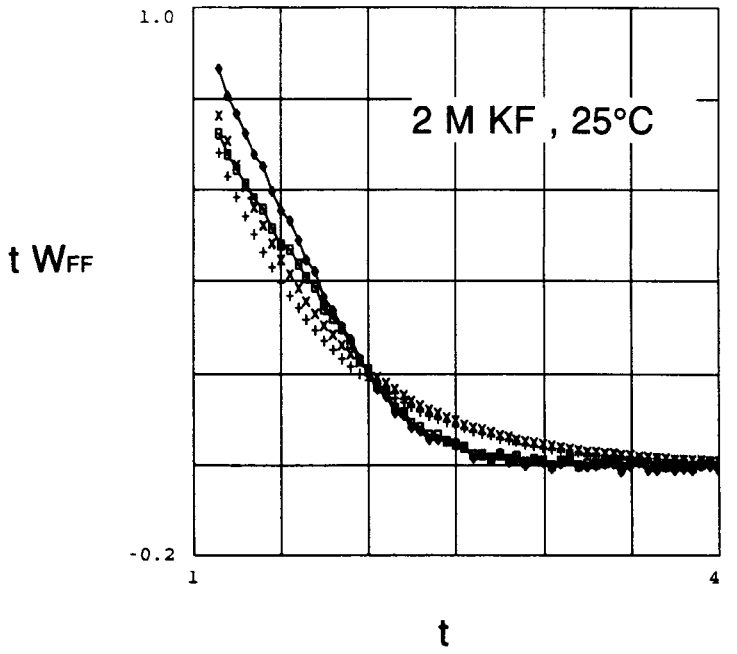

Figure 22 The dimensionless potential of mean forces (weighted by $t = r/a$) between F–F pairs in 2 M KF from MC simulations with $N = 1000$ ions. The rectangles are MC values, the + + + + are DHX values and the × × × × GDHX values. The diamonds are the "electric part" of the potential of mean forces. The "electric" potential of mean forces is further From DHX and GDHX near contact than the total potential of mean forces. The potential of mean forces converges more rapidly to zero than predicted by the (G)DHX theory.

Table 8 Contact values of the RDF's in 2 M KCl/KF solutions

Electrolyte	g^c_{KK}	g^c_{ClCl}	g^c_{FF}	g^c_{KCl}	g^c_{KF}	g^c_{ClF}
KCl	0.333 ± 0.003	0.333 ± 0.003	—	3.16 ± 0.03	—	—
KCl:KF = 12	0.322 ± 0.003	0.327 ± 0.005	?	3.15 ± 0.03	2.54 ± 0.04	0.407 ± 0.010
KCl:KF = 1	0.318 ± 0.003	0.324 ± 0.005	0.491 ± 0.005	3.18 ± 0.03	2.66 ± 0.03	0.410 ± 0.005
KF:KCl = 12	0.320 ± 0.010	?	0.496 ± 0.005	3.32 ± 0.03	2.68 ± 0.03	0.447 ± 0.020
KF	0.306 ± 0.003	—	0.512 ± 0.005	—	2.69 ± 0.03	—

The question marks refer to contact values between scarce ions, where the uncertainty and the N-dependence of the simulated values are both large. Reasonable estimates are $g^c_{ClCl} = 0.321$ for KF:KCl = 12 and $g^c_{FF} = 0.486$ for KCl:KF = 12.

It is seen, that the osmotic pressure increases linearly with increasing fraction of KF in the mixture. The reason is, that the fluoride ions have a larger excluded volume than the potassium ions the chloride ions. It is of especial interest that there is a pseudo-ideal point (where the osmotic pressure is given by the van't Hoff expression) at a certain salt

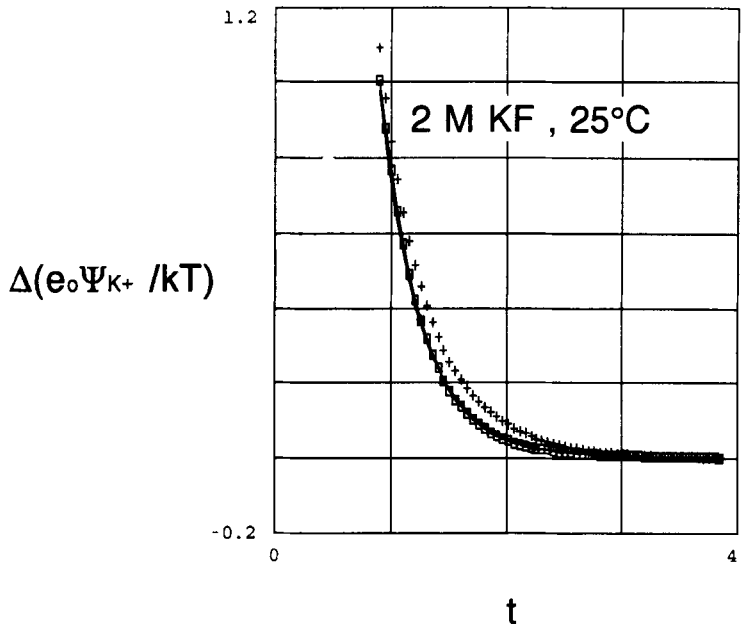

Figure 23 The dimensionless electric potential around a potassium ion in 2 M KF from MC simulations with $N = 1000$ ions. The rectangles are Poisson-integrated potentials from the simulated RDF's. Potentials are taken as differences relative to the potential at $t = r/a \approx 3.854$ (the mid point radius of the outermost spherical shell) but in practice the potential here may be put to zero. The + + + + curve is the Debye-Hückel potential. The solid curve fitting the MC values quite well is calculated from a DH expression with a $\kappa_{eff} = 1.27\,\kappa$.

Table 9 Excess osmotic pressure and the excess energy as a function of the salt fraction

X_{KF}	*0*	*1/13*	*1/2*	*12/13*	*1*
a(nm)	0.29	0.31666...	0.31666...	0.31666...	0.33
ρ^*	0.05876	0.07650	0.07650	0.07650	0.08658
CONTACT	0.2149	0.2179	0.2478	0.2798	0.2845
$E_{ex}/(3NkT)$	−0.2627	−0.2614	−0.2546	−0.2478	−0.2466
$\Pi_{ex}/(\rho_{tot}kT)$	−0.0477	−0.0435	−0.0068	+0.0320	+0.0380

fraction:

$$X_{KF}(\text{pseudo-ideal}) \approx 0.564 \tag{32}$$

There is a very slight indication of a curvature in the excess osmotic pressure vs. X_{KF}. Therefore, the best quadratic fit to the MC data is also given:

$$\Pi_{ex}/(\rho_{tot}kT) = -0.0486 + 0.0795\,X_{KF} + 0.0077\,X_{KF}^2 \tag{33}$$

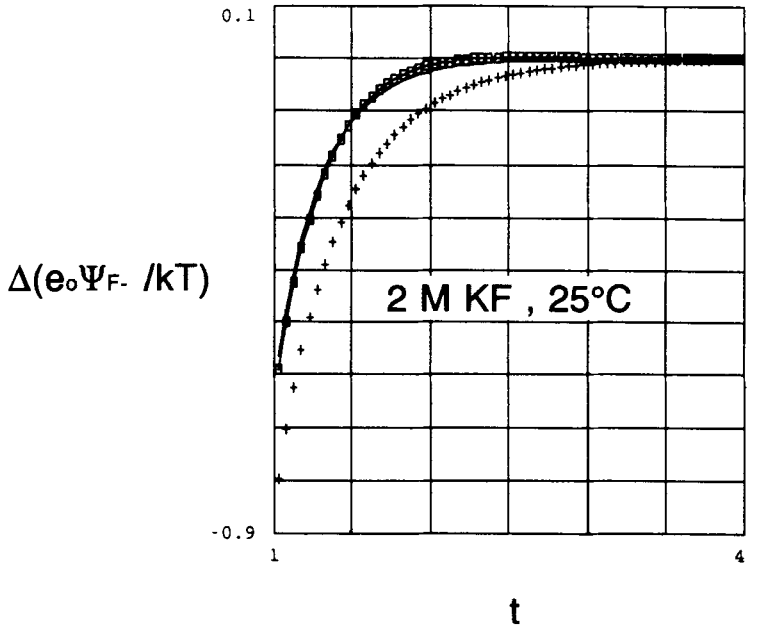

Figure 24 The dimensionless electric potential around a fluoride ion in 2 M KF from MC simulations with $N = 1000$ ions. The rectangles are Poisson-integrated potentials from the simulated RDF's. Potentials are taken as differences relative to the potential at $t = r/a \approx 3.975$ (the mid point radius of the outermost spherical shell) but in practice the potential here may be put to zero. The + + + + curve is the Debye-Hückel potential. The solid curve fitting the MC values quite well is calculated from a DH expression with a $\kappa_{eff} = 1.63\,\kappa$.

DISCUSSION

The variations of $\ln y_{Cl^-}$ and of $\ln y_{F^-}$ with the salt fraction are only ca. 14% and ca. 21% of the variation of $\ln y_{K^+}$ at 2 M total ionic strength according to Eqs. (12–14). At 1 M total ionic strength in the same system, it was similarly found in an earlier paper, that the variations of $\ln y_{Cl^-}$ and of $\ln y_{F^-}$ with the salt fraction were ca. 18% and ca. 2% of the variation of $\ln y_{K^+}$, see ref. [2], Eqs. 55–57. What is the reason for the much less variation in the excess chemical potentials of the two anions?

We must here distinguish between McMillan-Mayer excess chemical potentials (taken at the external pressure + the osmotic pressure) and Lewis-Randall excess chemical potentials (taken at constant pressure). The first are the ones found by Monte Carlo simulations of the primitive model. The primitive model assumes an effective pair potential modified by the solvent dielectric permitivity, and it is therefore a MacMillan-Mayer type of model with solvent averaged pair potentials. The Lewis-Randall excess chemical potentials are the ones found experimentally, however. In dilute solutions, the differences between the two sets of activity coefficients are negligible, but at the present concentrations the differences may be felt.

It is first made plausible, why the variation of the Lewis-Randall activity coefficients for K^+ is much greater than for Cl^- and F^-. Thereafter, the effect of the varying

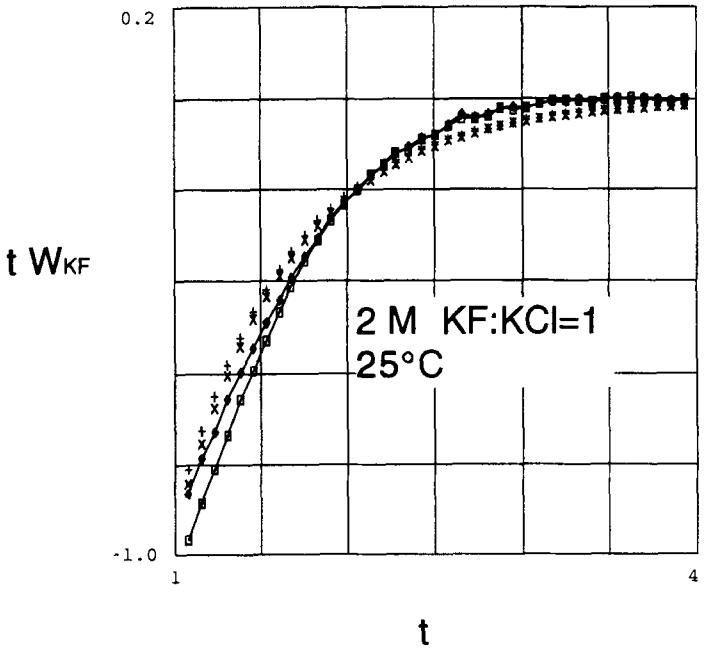

Figure 25 The dimensionless potential of mean forces (weighted by $t = r/a$) between K–F pairs in a mixture of 1 M KF and 1 M KCl from MC simulations with $N = 1000$ ions. The rectangles are MC values, the + + + + are DHX values and the × × × × GDHX values. The diamonds are the "electric part" of the potential of mean forces. The "electric" potential of mean forces is close to GDHX near contact. The potential of mean forces converges more rapidly to zero than predicted by the (G)DHX theory. (The mean radius $a = 0.31666...$ nm).

osmotic pressure with the salt fraction on the MacMillan-Mayer activity coefficients is discussed.

Let y_i be Lewis-Randall activity coefficients and let the temperature and pressure be constant. The first salt is called (1, 2) and the other salt (1, 3). For small variations in the number of ions we have:

$$\begin{aligned} d\ln y_1 &= \mu_{11}dN_1 + \mu_{12}dN_2 + \mu_{13}dN_3 \\ d\ln y_2 &= \mu_{12}dN_1 + \mu_{22}dN_2 + \mu_{23}dN_3 \\ d\ln y_3 &= \mu_{13}dN_1 + \mu_{23}dN_2 + \mu_{33}dN_3 \end{aligned} \tag{34}$$

The Maxwell symmetry has been introduced. Now consider a situation with a constant amount of the common ion (1), i.e. $dN_1 = 0$. Because of the electroneutrality we have $dN_2 = -dN_3 = dX_{12} = -dX_{13}$. Therefore:

$$d\ln y_1 = (\mu_{13} - \mu_{12})dX_{13} \tag{35a}$$

$$d\ln y_2 = (\mu_{23} - \mu_{22})dX_{13} \tag{35b}$$

$$d\ln y_3 = (\mu_{33} - \mu_{23})dX_{13} \tag{35c}$$

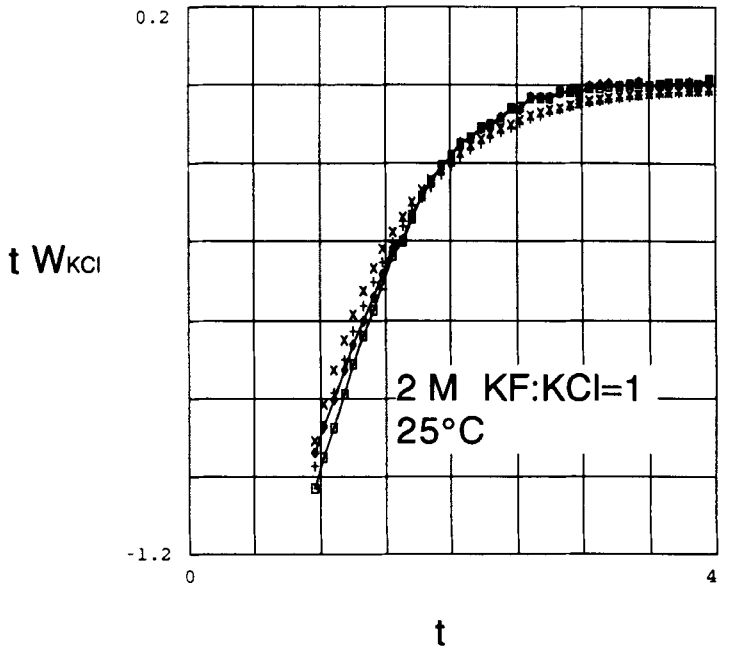

Figure 26 The dimensionless potential of mean forces (weighted by $t = r/a$) between K–Cl pairs in a mixture of 1 M KF and 1 M KCl from MC simulations with $N = 1000$ ions. The rectangles are MC values, the + + + + are DHX values and the × × × × GDHX values. The diamonds are the "electric part" of the potential of mean forces. The "electric" potential of mean forces is close to (G)DHX near contact. The potential of mean forces converges more rapidly to zero than predicted by the (G)DHX theory. (The mean radius $a = 0.316666...$ nm).

The μ_{ij}'s are generally functions of the ion concentrations. However, at 2 M total ionic strength, the differences $(\mu_{13} - \mu_{12})$, $(\mu_{23} - \mu_{22})$ and $(\mu_{33} - \mu_{23})$ seem to be independent of the salt fraction, so that the equations (35a–c) may be integrated to the linear Harned relations Eqs. (12–14).

For small values of the total ionic strength, there are only "nonspecific" energetic influences between the ions, *i.e.* through the square root of the common ionic strength. Since all ions contribute likely to the ionic strength, we have that $\mu_{13} - \mu_{12} \approx 0$, $\mu_{23} - \mu_{22} \approx 0$ and $\mu_{33} - \mu_{23} \approx 0$. (The quantities μ_{ij} are expected to be proportional to the ionic concentrations at small concentrations, so that they vanish before the square root influence at high dilution). There will be no dependence on salt fraction and no Harned coefficients. At higher total ionic strengths, "specific" effects dependent on the individual properties of the ions (here the diameters) come into play. The difference in sizes will only be much more important for two ions with a high probability of being in contact than for two ions with a low probability of contact. The common ion no. 1 (*e.g.* K^+) has opposite charge of the ions no. 2 and 3. The total concentrations of 2- and 3-ions around 1-ions are much higher than the bulk concentrations. Contrary to that, the specific interactions between 2-ions and 3-ions

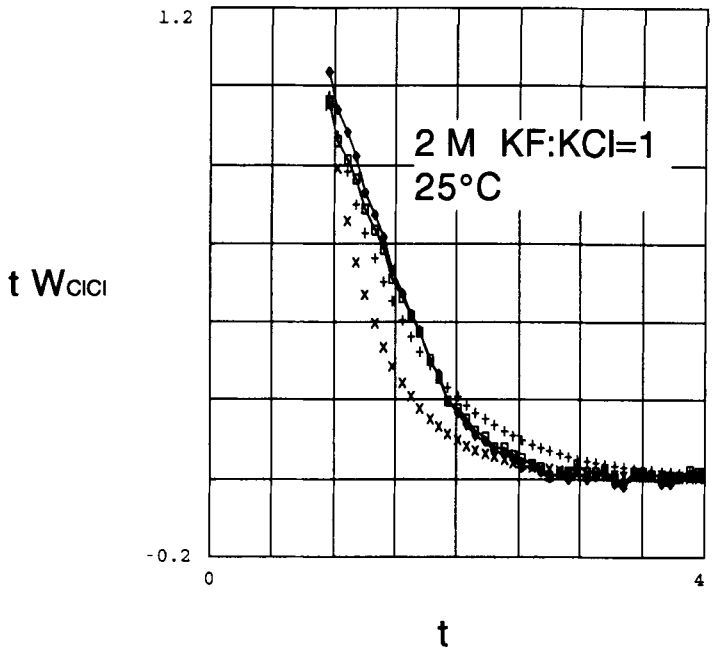

Figure 27 The dimensionless potential of mean forces (weighted by $t = r/a$) between Cl–Cl pairs in a mixture of 1 M KF and 1 M KCl from MC simulations with $N = 1000$ ions. The rectangles are MC values, the + + + + are DHX values and the × × × × GDHX values. The diamonds are the "electric part" of the potential of mean forces. The "electric" potential of mean forces is further from the (G)DHX values near contact than the total potential of mean forces. The potential of mean forces converges more rapidly to zero than predicted by the DHX theory, whereas the GDHX is better in the "tail". DHX is best in the intermediary range of t-values, however. (The mean radius $a = 0.316666...$ nm).

are very low, since they have the same charge and repel each other. The same is true for 2–2 pairs or 3–3 pairs. Therefore

$$|\mu_{13} - \mu_{12}| \gg |\mu_{23} - \mu_{22}| \text{ or } |\mu_{33} - \mu_{23}| \tag{36}$$

This explains the stronger dependence for K^+ on the salt fraction than for Cl^- and F^-. The chloride ion is in this study chosen much smaller than the fluoride ion. Thus, the repulsive energy between two chloride ions in contact is stronger than for a $Cl^- F^-$ pair, and the contact repulsion for this pair is again stronger than for a $F^- F^-$ pair. At the same time, the larger ions have the largest, positive "specific" influence on the chemical potential on another ion. These two effects act in the same direction. Therefore, we shall expect:

$$\mu_{13} - \mu_{12} \gg \mu_{33} - \mu_{23} > \mu_{23} - \mu_{22} > 0 \tag{37}$$

Therefore, the variation for the F^- ion is somewhat stronger than for the Cl^- ion. A "theory of specific interactions of ions" were introduced by Brønsted as early as 1921 (before the advent of the Debye-Hückel theory!) on the basis of experimental activity coefficient data [12]. Simplified formulations have been discussed by Guggenheim [13] and by Sørensen [14].

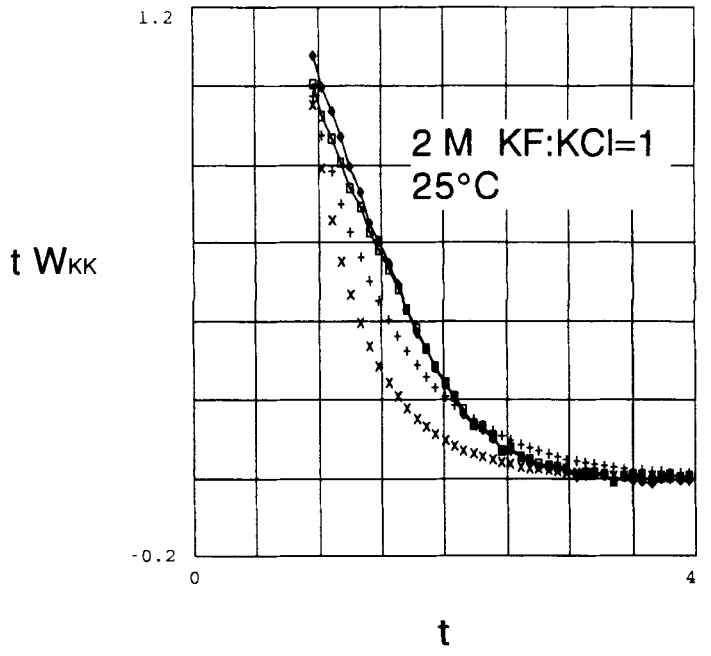

Figure 28 The dimensionless potential of mean forces (weighted by $t = r/a$) between K–K pairs in a mixture of 1 M KF and 1 M KCl from MC simulations with $N = 1000$ ions. The rectangles are MC values, the + + + + are DHX values and the × × × × GDHX values. The diamonds are the "electric part" of the potential of mean forces. The "electric" potential of mean forces is further from the (G)DHX values near contact than the total potential of mean forces. The potential of mean forces converges more rapidly to zero than predicted by the DHX theory, whereas the GDHX is better in the "tail". DHX is best in the intermediary range of t-values, however. (The mean radius $a = 0.316666...$ nm).

Next consider the influence of the variations in osmotic pressure. The pressure in a MacMillan-Mayer system follows the osmotic pressure. As shown by Eq. (31), the osmotic pressure increases almost linearly from a value slightly below the ideal pressure to a value slightly above with increasing content of KF in the mixture. The variation of the excess chemical potential of ion no. i with the increase in osmotic pressure is given by:

$$[\partial \mu_{ex,i}/\partial \Pi]_{T,N} = (\partial V_{ex}/\partial N_i)_{T,p,N_{j\neq i}} = v_{ex,i} \tag{38}$$

The excess, partial ionic volume (over and above the ideal value kT/Π) for ion no. i is called $v_{ex,i}$. The partial ionic volumes are expected to be positive at 2 M total ionic strength. Also, the partial volume should be larger for the fluoride ions than for the chloride ion. Thus, the increase in $\ln y_{F^-}$ (MM) with X_{KF} should be larger than the increase in $\ln y_{Cl^-}$(MM), where MM ~ MacMillan-Mayer. Thus, these effects act in the same direction as the effects already described for the LR-activity coefficients.

Guggenheim assumed, that there were no "specific interactions" between ions with charges of the same sign. This has been found not to be generally true for

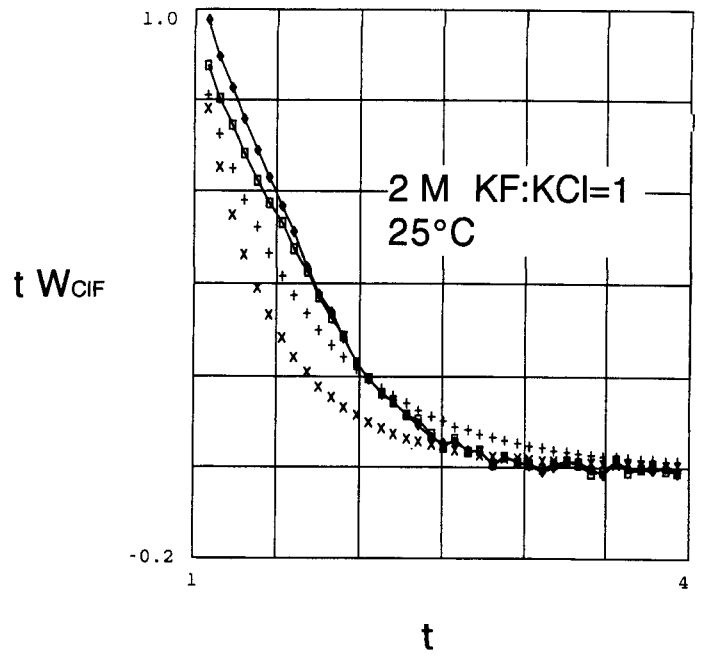

Figure 29 The dimensionless potential of mean forces (weighted by $t = r/a$) between Cl–F pairs in a mixture of 1 M KF and 1 M KCl from MC simulations with $N = 1000$ ions. The rectangles are MC values, the + + + + are DHX values and the × × × × GDHX values. The diamonds are the "electric part" of the potential of mean forces. The "electric" potential of mean forces is further from the (G)DHX values near contact than the total potential of mean forces. The potential of mean forces converges more rapidly to zero than predicted by the DHX theory, whereas the GDHX is better in the "tail". DHX is best in the intermediary range of t-values, however. (The mean radius $a = 0.316666\ldots$ nm).

ionic systems, but with this assumption upper limits of the excess, partial ionic volumes for the chloride and fluoride ions may be established assuming $v_{ex,i}$ to be independent of the salt fraction and comparing the coefficients in Eqs. (13–14) to the coefficient in Eq. (31):

$$v_{ex,Cl^-} \leqslant (0.31666\ldots 10^{-9})^3(0.0217)/[0.087{\cdot}0.07650] = 1.035{\cdot}10^{-28}\,\mathrm{m^3/ion} \quad (39)$$

$$v_{ex,F^-} \leqslant 1.60{\cdot}10^{-28}\,\mathrm{m^3/ion} \quad (40)$$

These figures might be compared to the ideal partial ionic volume:

$$v_{\text{ideal, any particle}} = kT/\Pi_{\text{ideal}} = (1/\rho_{\text{tot}})$$
$$= (0.31666\ldots 10^{-9})^3/0.07650 = 4.15{\cdot}10^{-28}\,\mathrm{m^3/ion} \quad (41)$$

The upper limits of the excess partial ionic volumes (39–40) are not unrealistically high compared to the ideal value.

Harned and Owen have given a thorough discussion of the thermodynamical implications of the Harned rule, see ref. [15], Chap. 14, section 5. Taking as the point of departure the linear rules of mixing for the mean activity coefficients of two electrolytes

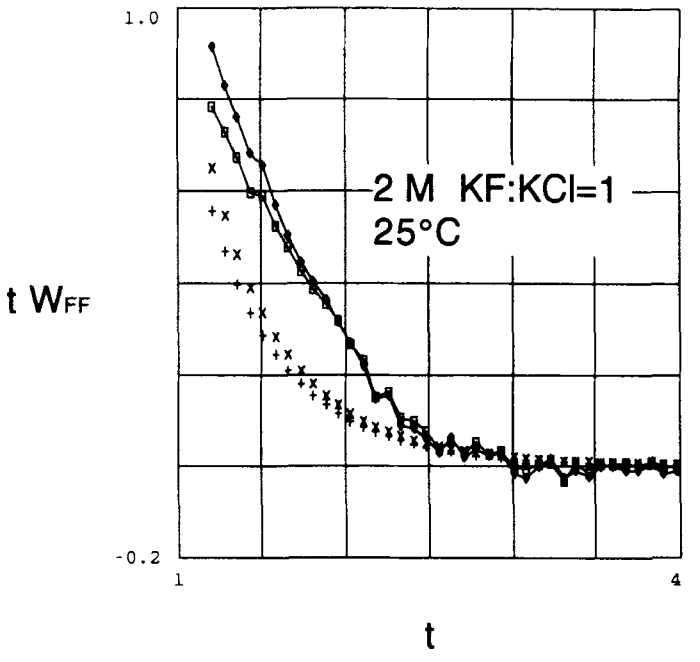

Figure 30 The dimensionless potential of mean forces (weighted by $t = r/a$) between F–F pairs in a mixture of 1 M KF and 1 M KCl from MC simulations with $N = 1000$ ions. The rectangles are MC values, the + + + + are DHX values and the × × × × GDHX values. The diamonds are the "electric part" of the potential of mean forces. The "electric" potential of mean forces is further from the (G)DHX values near contact than the total potential of mean forces. The DHX and GDHX are not very different, but both differ considerably from the simulated values. (The mean radius $a = 0.316666\ldots$ nm).

at total molarity $c(=c_1+c_2)$ and salt fraction X_1 of salt no. 1

$$\ln y_{\pm}(\text{salt 1}) = \ln y_{\pm}(\text{salt 1, pure}) - \alpha_{12}c_2 = \ln y_{\pm}(\text{salt 1, trace}) + \alpha_{12}c_1 \quad (42a)$$

$$\ln y_{\pm}(\text{salt 2}) = \ln y_{\pm}(\text{salt 2, pure}) - \alpha_{21}c_1 = \ln y_{\pm}(\text{salt 2, trace}) + \alpha_{21}c_2 \quad (42b)$$

one obtains for the excess osmotic coefficient (by differentiation with respect to the molalities using also the Gibbs–Duhem equation and integrating subsequently):

$$\{\Pi_{ex}(X_1) - \Pi_{ex}(X_1 = 0)\}/(cRT) = (c/2)\{(\alpha_{12}+\alpha_{21})X_1^2 - 2\alpha_{21}X_1\} \quad (43a)$$

$$\{\Pi_{ex}(X_2) - \Pi_{ex}(X_2 = 0)\}/(cRT) = (c/2)\{(\alpha_{21}+\alpha_{12})X_2^2 - 2\alpha_{12}X_2\} \quad (43b)$$

Especially one has:

$$\alpha_{21} - \alpha_{12} = (2/c)\{\{\Pi_{ex}(\text{pure 2}) - \Pi_{ex}(\text{pure 1})\}/(cRT)\} \quad (44)$$

(We have replaced molality by molarity and molal mean ionic activity coefficients by mean molar activity coefficients). Harned and Owen distinguish four different cases:

(I) General case: The $\ln y_{\pm}$'s exhibit Harned linearity, $\alpha_{12}+\alpha_{21} \neq 0$ and the osmotic coefficient vs. salt fraction plot is curved according to (43a, b). The trace activity coefficients of the two salts are generally different.

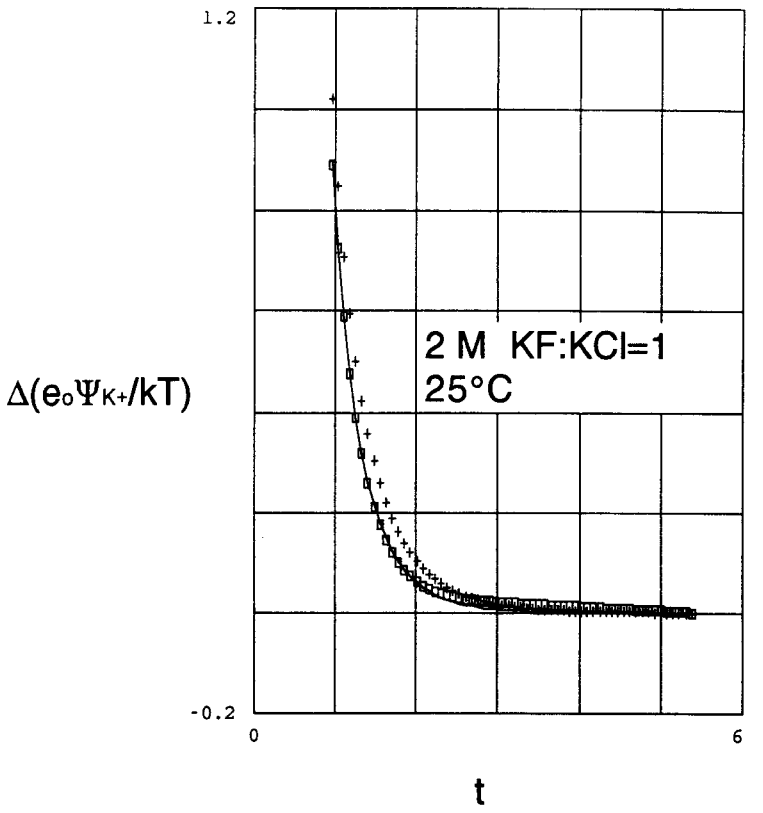

Figure 31 The dimensionless electric potential around a potassium ion in a mixture of 1 M KF and 1 M KCl from MC simulations with $N = 1000$ ions. The rectangles are Poisson–integrated potentials from the simulated RDF's. Potentials are taken as differences relative to the potential at $t = r/a \approx 5.3783$ but in practice the reference potential may be set to zero. The + + + + curve is the Debye-Hückel potential. The solid curve fitting the MC values quite well is calculated from a DH expression with a $\kappa_{eff} = 1.27\,\kappa$.

(II) Åkerlöf case: The so-called Åkerlöf-Thomas relation (again taking c instead of m)

$$\ln y_{\pm}(\text{pure 1 at } c) - \ln y_{\pm}(\text{pure 2 at } c) \approx B_{12}c \tag{45}$$

is empirically shown to be approached at high concentrations for many electrolytes with B_{12} independent of concentration. It may then be shown, that

$$\alpha_{12} - \alpha_{21} = B_{12} \tag{46}$$

and

$$y_{\pm}(\text{salt 1, trace}) = y_{\pm}(\text{salt 2, trace}) \tag{47}$$

(III) Brønsted case: In Brønsted's theory of specific interactions, ions of unlike sign influence the chemical potential of each other in a specific way, while ions of the same sign have identical influence on each other. Apart from that, each ion has a characteristic "salting out coefficient" acting upon all the other ions in the solution. A consequence

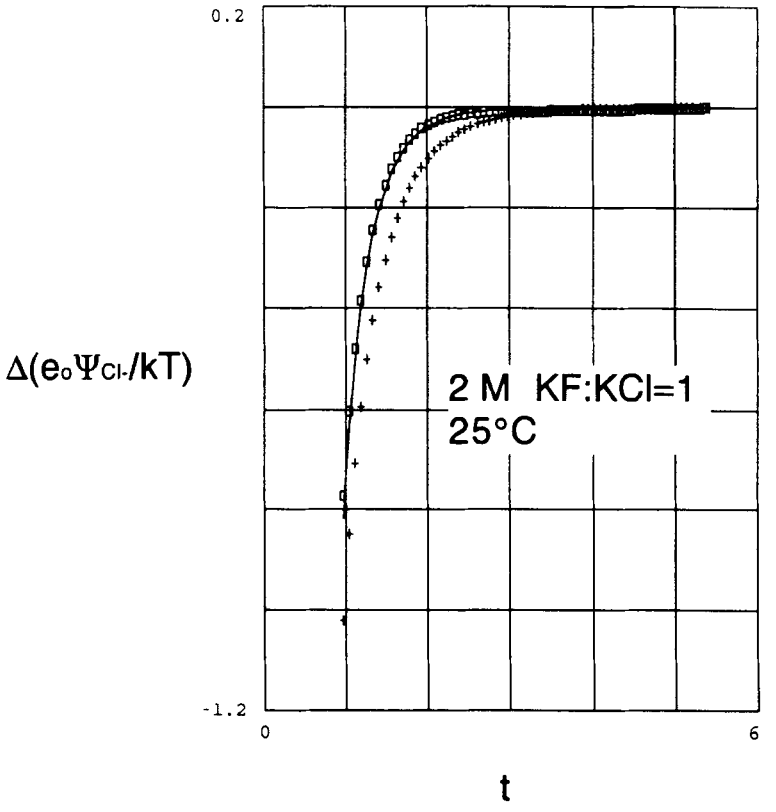

Figure 32 The dimensionless electric potential around a chloride ion in a mixture of 1 M KF and 1 M KCl from MC simulations with $N = 1000$ ions. The rectangles are Poisson-integrated potentials from the simulated RDF's. Potentials are taken as differences relative to the potential at $t = r/a \approx 5.3783$ but in practice the reference potential may be set to zero. The + + + + curve is the Debye-Hückel potential. The solid curve fitting the MC values quite well is calculated from a DH expression with a $\kappa_{eff} = 1.50\,\kappa$.

of this theory is that

$$\alpha_{12} + \alpha_{21} = 0 \tag{48}$$

and the the osmotic pressure is strictly linear in the salt fraction. The trace activity coefficients are generally different.

(IV) Guggenheim case: In the simplified theory of specific interactions of ions of Guggenheim, the salting out coefficients are neglected. Eq. (48) is valid, so the osmotic pressure is strictly linear in the salt fraction. The Åkerlöf-Thomas relation can be derived from the Guggenheim theory. Thus, the trace activity coefficients are equal to each other and can be calculated from the activity coefficients of the pure electrolytes:

$$\ln y_{\pm}(1, \text{trace}) = \ln y_{\pm}(2, \text{trace}) = [\ln y_{\pm}(1, \text{pure}) + \ln y_{\pm}(2, \text{pure})]/2 \tag{49}$$

Harned and Owen also derives the McKay relation from Maxwell cross differentiation, [15], Chap. 14, section 10. For 1:1 electrolyte mixtures this relation states that

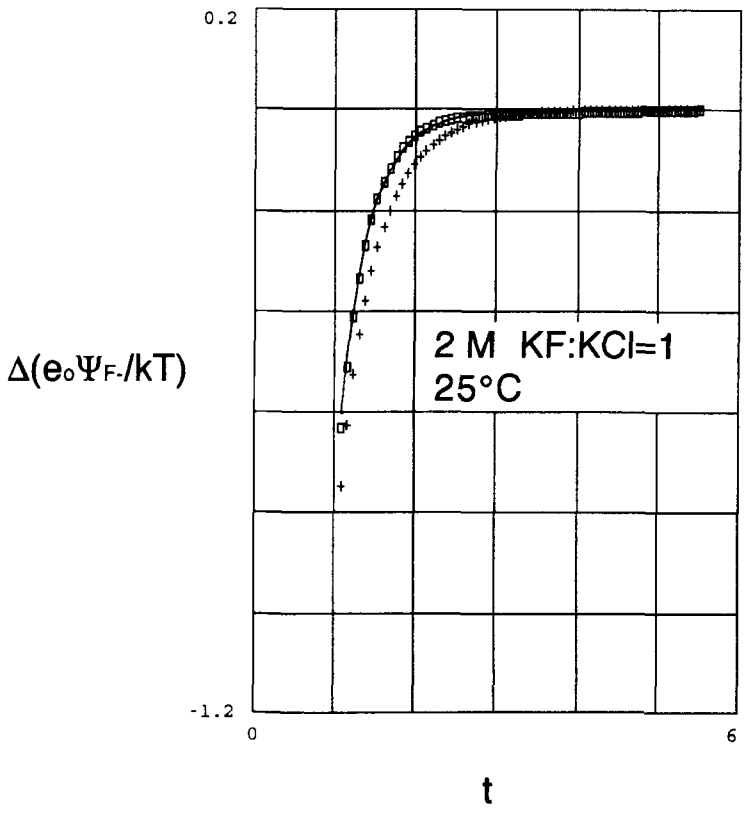

Figure 33 The dimensionless electric potential around a fluoride ion in a mixture of 1 M KF and 1 M KCl from MC simulations with $N = 1000$ ions. The rectangles are Poisson-integrated potentials from the simulated RDF's. Potentials are taken as differences relative to the potential at $t = r/a \approx 5.5046$ but in practice the reference potential may be set to zero. The + + + + curve is the Debye-Hückel potential. The solid curve fitting the MC values quite well is calculated from a DH expression with a $\kappa_{eff} = 1.33\,\kappa$.

$$\alpha_{12} + \alpha_{21} = \text{constant (independent of total concentration)} \qquad (50)$$

As a special case, $\alpha_{12} + \alpha_{21}$ may be zero at all concentrations as in the theories of specific ion interactions of Brønsted and of Guggenheim.

In Table 10 some of the thermodynamic relations are checked for the simulated system using also some data for 1 M total concentrations from ref. [2].

From Table 10 it is apparent that $\alpha_{12} + \alpha_{21}$ is not independent on concentration. However, the present simulations at 2 M are much more extended (longer runs and more N-values) than the simulations at 1 M described in refs. [1–2]. Since α_{21} *is positive and* α_{12} *is negative and* $\approx \alpha_{21}$ (the osmotic pressure is linear in the salt fraction or very nearly so), there is a large relative error in $\alpha_{12} + \alpha_{21}$. The value might be zero. The value $0.012\,\mathrm{L\,mol^{-1}} \gg 0.0048\,\mathrm{L\,mol^{-1}}$ might just be a reflection of a more "uncertain zero" at 1 M. The Åkerlöf-Thomas relation is quite

Table 10 Thermodynamic relations in simulated KCl (1)/KF (2) mixtures

c mol L^{-1}	$\alpha_{12}+\alpha_{21}$ L mol^{-1}	B_{12} L mol^{-1}	$\alpha_{21}-\alpha_{12}$ L mol^{-1}	$(2/c)\{\Pi_{ex}(KF)-\Pi_{ex}(KCl)\}/(cRT)$ L mol^{-1}
1.0	0.012	−0.096	+0.082	—
2.0	0.0048	−0.0945	+0.0920	+0.0857

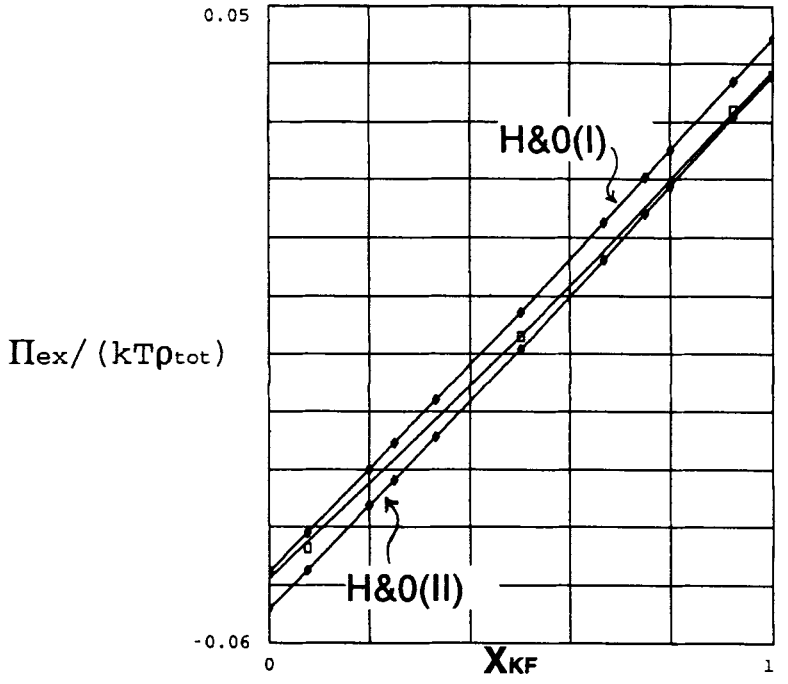

Figure 34 The dimensionless excess osmotic pressure (= the osmotic coefficient) as a function of the fraction of KF in a 2 M KCl–KF mixture. The rectangles are calculated from MC simulations, and the best fitting second order polynomial in the salt fraction (solid curve) is calculated from Eq. (33). The two Harned and Owen curves (diamonds) are calculated from the expressions (43a) and (43b). There is a pseudo-ideal point with ideal van't Hoff osmotic pressure at a salt fraction $X_{KF} \approx 0.564$.

well obeyed, however, since B_{12} is practically independent of the concentration. The relation (46) is approximately obeyed – best at 2 M total concentration. The trace activity coefficients should then be approximately equal, which they are at both 1 M and 2 M – although the difference between trace activity coefficients seems statistical significant at both concentrations. The relation (44) is only obyed very approximately (at 2 M). The same imprecision is demonstrated in Figure 34 showing the osmotic coefficient vs. the fraction of KF in the mixture. The rectangles are the MC values, the curve is the quadratic fit (33) and the curves with diamonds are the two equations (43a) and (43b). The uncertainty reflects probably mostly the fact that the activity coefficients simulated were MacMillan-Mayer and not Lewis-Randall coefficients.

From the above considerations it can be concluded, that the simulated system is close to being a case (IV) system with X-linear osmotic coefficient, with $\alpha_{12} = -\alpha_{21}$ and with equal trace activity coefficients. Furthermore, the single ion activity coefficients for Cl^- and F^- vary much less with the salt fraction than the coefficient for K^+.

In Table 11 Mean Spherical Approximation values are compared to the MC values at 1 M and 2 M total concentration. The deviation of the MSA values from the true values are generally at the second significant digit at 2 M and at the third (sometimes the second) significant digit at 1 M. The values of the osmotic coefficient near the pseudo-ideal point are of less precision – of course – but the MSA theory spots quite well the pseudo-ideal point. The relative simplicity of the MSA theory taken into account, the semi-quantitative agreement of the theory is quite impressive. It may be used in surveys, but not for precision work.

The MSA theory is isomorphous with the simple Debye–Hückel theory with 2Γ replacing κa in the case of two ions of the same size and opposite charge. For example one has

$$E_{ex}/NkT = (-B/2)(2\Gamma)/(1 + 2\Gamma] \tag{51}$$

and

$$2\Gamma a = [x + 1 - \sqrt{(1 + 2x)}]/[\sqrt{(1 + 2x)} - (x/2) - 1] \quad (x \equiv \kappa a) \tag{52}$$

For different ionic radii, the value of Γ must be found numerically [11]. Since $2\Gamma a \to \kappa a$ for $\kappa a \to 0$, the two theories yield identical results at high dilution. The MSA is better than the DH-theory in the way, that it does not only treat the selected "central ion" to

Table 11 Comparison between MSA and MC values at 1 M and 2 M total concentration

X_{KF}:		*0*	*1/13*	*1/2*	*12/13*	*1*	*c*
E_{ex}/NkT	MSA	−0.64106	−0.63850	−0.62449	−0.61083	−0.60842	1 M
	MC	−0.6553	−0.6514	−0.6363	−0.6196	−0.6157	1 M
	MSA	−0.77664	−0.77303	−0.75363	−0.73470	−0.73133	2 M
	MC	−0.78868	−0.78314	−0.76493	−0.74249	−0.74011	2 M
$\Pi_{ex}/\rho kT$	MSA	−0.04408	−0.03759	−0.000438	+0.0392	+0.0467	2 M
	MC	−0.0477	−0.0435	−0.0068	+0.0320	+0.0380	2 M
$\ln y_{K^+}$	MSA	−0.5144	−0.5081	−0.4734	−0.4383	−0.4320	1 M
	MC	−0.518	−0.512	−0.478	−0.438	−0.420	1 M
	MSA	−0.5156	−0.5040	−0.4395	−0.3740	−0.3620	2 M
	MC	−0.5228	−0.5140	−0.4493	−0.3763	−0.3690	2 M
$\ln y_{Cl^-}$	MSA	−0.5144	−0.5139	−0.5113	−0.5084	−0.5079	1 M
	MC	−0.518	−0.515	−0.527	−0.531	−0.533	1 M
	MSA	−0.5156	−0.5143	−0.5065	−0.4979	−0.4963	2 M
	MC	−0.5228	−0.5253	−0.5203	−0.5102	−0.5087	2 M
$\ln y_{F^-}$	MSA	−0.4107	−0.4099	−0.4048	−0.3994	−0.3985	1 M
	MC	−0.416	−0.416	−0.417	−0.417	−0.418	1 M
	MSA	−0.3269	−0.3244	−0.3094	−0.2934	−0.2904	2 M
	MC	−0.3392	−0.3368	−0.3224	−0.3073	−0.3067	2 M

MSA values of the thermodynamic parameters calculated according to Ref. [11].

have an extension, but also the ions in the ionic cloud in a symmetric manner, see Blum [16]. In the MSA theory the RDF's are linearized near the ions as in the DH theory, so that the MSA does not yield good RDF's near contact. In the case of 2 M KCl, we calculate $2\Gamma a/\kappa a = 1.2702$ and $E_{ex}/NkT = -0.77664$, see also Table 11. The "effective" value of κ found from the electric potentials derived from MC simulations. (Table 7) was a factor 1.38 ± 0.03 greater than the DH value of κ. Thus, 2Γ is not far from κ_{eff}. However, Table 7 also shows, that in general, there are different values of κ_{eff} – one belonging to each ion – and not just a common value 2Γ. Therefore, the MSA picture is fundamentally too naive.

The analysis of the simulated RDF's showed, that the inverse Debye length is still dominating the behaviour even at 2 M total concentration, where this length is considerably smaller than the smallest ions in the mixture. However, the DHX or "generalized" DHX approximation works less well than at 1 M. In general, the GDHX potentials of mean forces were not better than DHX at 2 M (often worse). The simulated potentials of mean forces also vanish more rapidly than the (G) DHX potentials of mean force, when the ion separation increases. The electric potentials around each of the ions follow approximately from a DH-like equation with an effective inverse Debye length for each ion (Table 7), which is larger than the DH screening length. (This is well in accordance with the fact that the potentials of mean forces vanish more rapidly than DHX). Apart from that, it is difficult to observe any pattern in the effective κ-values in Table 7, although it is observed that in a 2 M pure KF solution one has:

$$4.41(\text{nm})^{-1} = \kappa_{eff}(F^-)/\kappa a_{F^-F^-} \approx \kappa_{eff}(K^+)/\kappa a_{K^+K^+} = 4.38(\text{nm})^{-1} \qquad (53)$$

Thus for a two-ion system at 2 M, the effective screening lengths seem to be inversely proportional to the ion diameter. The 1:1 KF/KCl mixture seems to be much more complicated to describe, however. Here the K^+ ion has approximately a screening length as K^+ in a 2 M KF solution, whereas the Cl^- ion with the same size as the K^+ ion has a much shorter screening length. The F^- ion has a screening length midway between the screening length of the Cl^- ion in a 2 M KCl solution and the K^+ ion in a 2 M KF solution.

A final observation should be noticed in onnection with the simulation of the RDF's of chargeless hard sphere systems, since it may also have some implications for the simulation of ionic systems. Figure 35 shows the RDF's in a hard sphere "KCl" system at 2 M (with chargeless "ions" of diameter 0.29 nm). Since the same computer program is used as for ionic systems (setting $B = 0$), an artificial division is performed into g_{KCl} and $g_{KK} = g_{ClCl} = g_A$ even if the particles are perfectly identical spheres. The RDF's are sampled as local concentrations in 60 spherical shells around the ions, and then divided by half of the total concentration of ions in the bulk. In the case of g_{KCl} this does not lead to any problems, since the particles counted are from a different group of particles than the "central particles". In the case of g_A, however, one ion is constantly missing in the counting *viz.* the central ion itself. When normalizing with the bulk ionic concentration of this group of ions, one obtains values of g_A which are systematically too low.

The broken line with rectangles in Figure 35 are MC results for g_{KCl} with $N = 1000$ and they should be very close to the true RDF in such a "monodisperse" hard spheresystem. It is seen, that the significant deviations from unity are located within

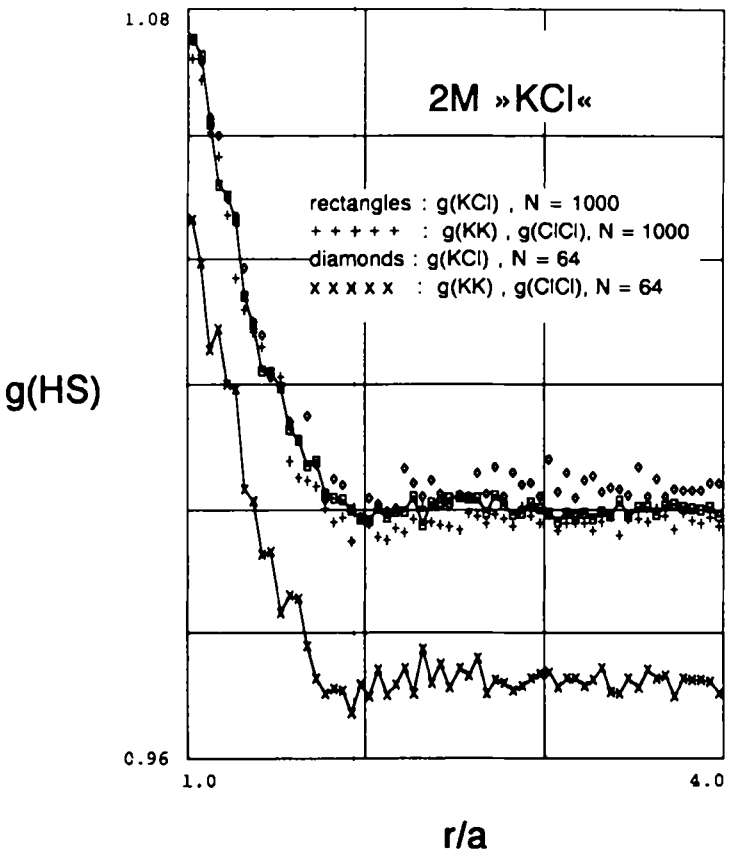

Figure 35 Simulated radial distribution functions in a hard sphere system corresponding to 2 M chargeless"KCl", $B = 0$ and $\rho^* = 0.05876$. The same programme is used as for charged particles. Therefore, the K- and Cl-particles may be artificially distinguished even if they are in reality indistinguishable. For $N = 1000$ the values of $g_{KK} = g_{ClCl} = g_A$ (symbol + + + +) are slightly lower than the values of g_{KCl} (rectangles on broken line). For $N = 64$, g_{KCl} (diamonds) is somewhat too high in the "tail", but g_A (× × × ×) is drastically too low at all values of r/a. This is so, since *e.g.* a K-particle only counts a total of 31 other K-particle in the simulation cell. Thus, the effective concentration is only the fraction 31/32 of $\rho^*/2$. In the programme, however, the RDF's are normalized by division by $\rho^*/2$.

one diameter separation from contact. After this, the broken curve fluctuates narrowly around unity. The + + + points are MC data for g_A with $N = 1000$, and it is seen that they are slightly displaced below unity in the "tail" of the distribution. The diamonds are MC data for g_{KCl} with $N = 64$, and they are perfectly identical to g_{KCl} with $N = 1000$ near contact, but somewhat too high in the "tail". However, the MC data for g_A with $N = 64$ are drastically too low at all separations. This is so, since a K-particle for example always "sees" only 31 other K-particles around and not 32.

This may be remedied by simply correcting the values of g_A by the factor 32/31 or more generally by $(N/2)/[(N/2) - 1]$. Figure 36 shows the result. Near contact, all four RDF's seem now statistically identical. In the "tail", the corrected MC data for g_A for

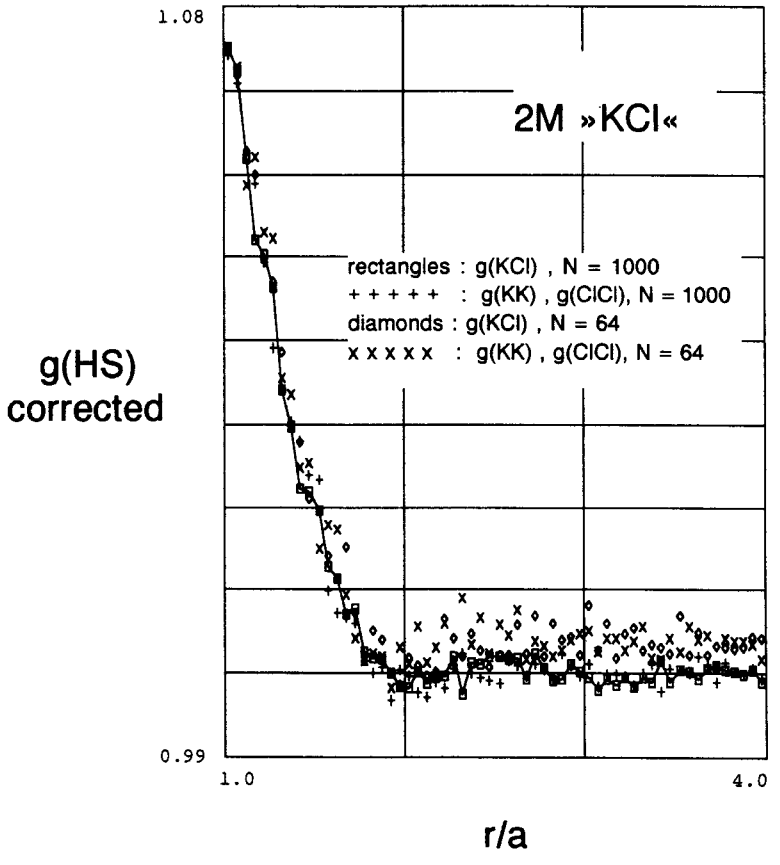

Figure 36 The same RDF's as in Figure 35, but the values of g_A have been corrected multiplying by the factor 500/499 (for $N = 1000$) and by 32/31 (for $N = 64$). The two RDF's for $N = 1000$ are now statistically identical in the whole range of r/a values. The "hard sphere attraction" has vanished after one diameter from contact. At greater separations g_{KCl} (rectangles on broken line) as well as g_A fluctuate narrowly around unity. The two RDF's for $N = 64$ are now also statistical identical, and they are identical to the values for $N = 1000$ close to contact. In the "tail", however, the $N = 64$ values are both systematically two high. This effect must be stemming from the periodic boundary conditions alone (minimum image energy cut-off has no importance for a hard sphere system). The corrections made here for a hard sphere system should be applied also to RDF's between ions of the same sort in MC simulations of electrolyte systems.

$N = 1000$ (+ + +) now fluctuates narrowly around unity. The values of g_{KCl} (diamonds) and of g_A(× × ×) for $N = 64$ are now statistically identical in the "tail", but both are higher than unity. This deviation is a true measure of the influence of the periodic boundary conditions in the system.

The same considerations are true in ionic systems. The values of g_{ii} for ions of type i should really be "corrected" by the factor $N_i/(N_i - 1)$. For large values of N_i's, the correction is insignificant. However, in high precision MC the deviation may still be observed for quite large numbers of ions in the simulation box. For example $G_0(r) \equiv \sqrt{(g_{+-} \cdot g_A)}$ was plotted for a very dilute 2:2 electrolyte with ions of equal size in Ref. [2], Fig. 5 for a total number of ions $N = 1728$. In the "tail" a clear depression

below unity was seen, and the value of $G_0(r)$ fluctuated around ca. 0.9995. The value of $\sqrt{(863/864)}$ is ca. 0.99942.

In the present study, the mentioned correction is mostly of very small importance. The correction factor is largest in the 1:1 mixtures with F – F and Cl – Cl pairs, namely 250/249 (since a total of 1000 ions were used). The electric potentials around the three ions (Figures 31–33) were somewhat affected by the correction (the integrated MC data moved closer to the Debye-Hückel curve) and indeed, the data marked as rectangles and diamonds in these figures were calculated using the correction. The potential of mean forces between to fluoride ions in an 1:1 mixture (Figure 30) was very slightly affected in the "tail", and the data shown are the corrected ones. In all the other cases, the consequences of performing the correction were not visible in the plots.

References

[1] T.S. Sørensen, J. Jensen and P. Sloth, "Experimental activity coefficients in aqueous mixed solutions of KCl and KF at 25°C compared to Monte Carlo Simulations and Mean Spherical Approximation Calculations", *J. Chem. Soc., Faraday Trans.*, **85** (1), 2649 (1989).

[2] T.S. Sørensen, "High precision canonical ensemble Monte Carlo simulations of very dilute, primitive Z:Z and 2:1 electrolytes and of moderately concentrated 1:1 electrolyte mixtures", *Molecular Simulation*, **11**, 1 (1993).

[3] T.S. Sørensen, "Direct calculation of the electri potential around ions from high precision canonical ensemble Monte Carlo simulations of some primitive model electrolyte systems", *Molecular Simulation*, **11**, 267 (1993).

[4] D.N. Card and J.P. Valleau, "Monte Carlo study of the thermodynamics of electrolyte solutions" *J. Chem. Phys.*, **52**, 6232 (1970).

[5] B. Widom, "Some topics in the theory of fluids" *J. Chem. Phys.*, **39**, 2808 (1963).

[6] B. Widom, "Potential-distribution theory and the statistical mechanics of fluids" *J. Chem. Phys.*, **86**, 869 (1982).

[7] T.S. Sørensen, "Error in the Debye-Hückel approximation for dilute primitive model electrolytes with Bjerrum parameters of 2 and *ca.* 6.8 investigated by Monte Carlo Methods: Excess energy, Helmholtz free energy, heat capacity and Widom activity coefficients corrected for neutralising background" *J. Chem. Soc. Faraday Trans.*, **87**, 479 (1991).

[8] T.S. Sørensen, "How wrong is the Debye-Hückel approximation for dilute primitive model electrolytes with moderate Bjerrum parameter?" *J. Chem. Soc. Faraday Trans.*, **86**, 1815 (1990).

[9] T.S. Sørensen, "Ions in solution and in weak ion exchange membranes" in *Capillarity Today. Lecture Notes in Physics, Vol. 386*, G. Pétré and A. Sanfeld, eds., Springer-Verlag, Berlin–Heidelberg–New York– London–Paris–Tokyo–Hong Kong–Barcelona-Budapest, 1991, pp. 164–221.

[10] T.M. Reed and K.E. Gubbins, *Applied Statistical Mechanics*, McGraw-Hill, New York, 1973.

[11] W. Ebeling and K. Scherwinski, "On the estimation of theoretical individual activity coefficients of electrolytes. I. Hard sphere model", *Z. physikal. Chem.* (Leipzig) 264, 1 (1983).

[12] J.N. Brønsted, "The principle of the specific interaction of ions", *Kgl. Danske Videnskab. Selskab, Mat.-Fys. Medd.* **IV**, 4 (1921).

[13] E.A. Guggenheim, *Thermodynamics*, North-Holland Publishing Co., Amsterdam, 1959.

[14] T.S. Sørensen, "Brønsted's principle of specific interaction of ions and the mean ionic activity coefficients in aqueous solutions of earth alkali halogenides Calculation of cationic radii from the ASPEV theory" *Acta Chem. Scand.* **A33**, 583 (1979).

[15] H.S. Harned and B.B. Owen, *The Physical Chemistry of Electrolytic Solutions*, 3rd Ed., Reinhold Publishing Corp., New York, 1958.

[16] L. Blum, "Primitive Electrolytes in the Mean Spherical Approximation" *Theoretical Chemistry: Advances and Perspectives* **5**, 1 (1980).